EUROPEAN ORGANIZATION FOR NUCLEAR RESEARCH (CERN)

CERN-EP-2023-213
2023/11/01

CMS-B2G-20-012

Search for W′ bosons decaying to a top and a bottom quark in leptonic final states in proton-proton collisions at $\sqrt{s} = 13\,\text{TeV}$

The CMS Collaboration*

Abstract

A search for W′ bosons decaying to a top and a bottom quark in final states including an electron or a muon is performed with the CMS detector at the LHC. The analyzed data correspond to an integrated luminosity of 138 fb^{-1} of proton-proton collisions at a center-of-mass energy of 13 TeV. Good agreement with the standard model expectation is observed and no evidence for the existence of the W′ boson is found over the mass range examined. The largest observed deviation from the standard model expectation is found for a W′ boson mass ($m_{\mathrm{W}'}$) hypothesis of 3.8 TeV with a relative decay width of 1%, with a local (global) significance of 2.6 (2.0) standard deviations. Upper limits on the production cross sections of W′ bosons decaying to a top and a bottom quark are set. Left- and right-handed W′ bosons with $m_{\mathrm{W}'}$ below 3.9 and 4.3 TeV, respectively, are excluded at the 95% confidence level, under the assumption that the new particle has a narrow decay width. Limits are also set for relative decay widths up to 30%. These are the most stringent limits to date on this W′ boson decay channel.

Submitted to the Journal of High Energy Physics

*See Appendix B for the list of collaboration members

1 Introduction

Despite the remarkable success of the standard model (SM), it is not a complete theory since it is not able to explain several experimental observations. Among the notable phenomena that may require the existence of physics beyond the SM are the apparent existence of dark matter, the matter-antimatter asymmetry in the universe, and neutrino oscillations. The SM also does not provide an explanation for the origin of its internal structure, such as the hierarchy of fermion masses, and suffers from the fine-tuning problem, which reflects the need to keep quantum corrections to the Higgs boson mass finite. All of these phenomena suggest the existence of a more fundamental theory.

Many models have emerged to provide an explanation for these open issues, often introducing new particles in the energy range reachable at the CERN Large Hadron Collider (LHC). Several of these models predict the existence of new massive bosons, called W' and Z', with similar properties to their SM counterparts, the W and Z bosons, respectively, that act as mediators of the electroweak interaction [1–15].

Models with W' and Z' bosons, coupled preferentially to third-generation fermions, are of particular interest as they could be involved in the explanation of flavor anomalies [16–18], or in the mechanism of electroweak symmetry breaking [19, 20]. In this context, the top quark plays a particularly important role, as it has both a large Yukawa coupling to the Higgs boson and a distinctive experimental signature due to its decay chain. Dedicated searches for W' and Z' bosons coupled preferentially to third-generation quarks and leptons have been performed in the past by both the CMS and ATLAS Collaborations [21–25]. No significant evidence for the existence of these particles has been found.

In this paper we present a search for a W' boson decaying to a top and a bottom quark, targeting the high end of the accessible mass spectrum at the LHC in the multi-TeV range. The analysis focuses on the decay chains of the hypothesized W' boson including leptons, i.e., $W' \to tb \to Wbb \to \ell\nu bb$, where ℓ represents either an electron or a muon, including the leptonic decays of the τ lepton. A representative leading-order (LO) Feynman diagram of the process considered here is shown in Fig. 1.

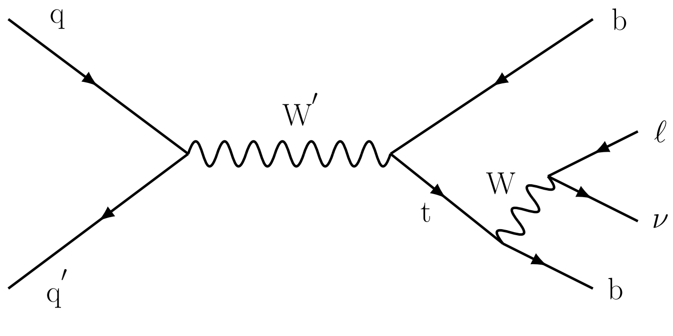

Figure 1: Representative LO Feynman diagram for a W' boson produced in the s-channel and decaying to a top and a bottom quark, with a lepton in the final state.

Hypotheses for the new particle mass, $m_{W'}$, are considered in the range 2-6 TeV, and the analysis strategy is tailored towards reconstructing highly energetic top quarks with a lepton in the final state, complementing previous searches in the range below 3 TeV [21, 25]. Different hypotheses for the width as well as the chirality of the new particle are explored to allow for an interpretation in a wide array of models.

Depending on the model, the relative decay width of the W′ boson with respect to its mass ($\Gamma/m_{\mathrm{W}'}$) could be significant [12, 20, 26, 27], resulting in signatures that could escape standard searches. This analysis probes $\Gamma/m_{\mathrm{W}'}$ of 1, 10, 20, and 30%, for the first time. The total width of approximately 1% (more precisely 0.8%) corresponds to the case where the W′ boson is only allowed to decay into t and b quarks. In the model used here, the couplings, and thus the partial widths, are kept fixed and not varied together with the total width. In this interpretation, the larger width can be attributed to the presence of additional decays, as several models predict W′ bosons decaying to additional new particles [26, 27]. This leads to a reduced branching fraction compared to only considering W′ → tb decays. We consider cases where the chirality of the W′ boson is left-handed (LH), right-handed (RH), or a combination of the two. For the LH, the signal is simulated including the SM production of single top quarks in the *s*-channel and the relative interference with the production with the W′ boson, which leads to a different signal phenomenology, depending on the mixing of the chiral components.

Figure 2 shows representative distributions of the mass of the system composed of the top-bottom quark pair as originating from the W′ boson for narrow- and large-width samples, for left- and right-handed chiralities, respectively, for a W′ boson mass of 3.6 TeV.

The width of the W′ boson affects the reconstructed mass distribution, resulting in a broader peak and an asymmetry favoring lower values. This is quite visible for the cases with large decay width, where the tail towards small masses is dominant because of off-shell W′ boson production, enhanced by rapidly increasing parton distribution functions (PDFs) for decreasing partonic momentum fractions. For the left-handed hypothesis, the region of the $m_{\mathrm{W}'}$ spectrum below 2 TeV is dominated by the SM *s*-channel single top quark production, yielding a very different signal shape compared to the RH case.

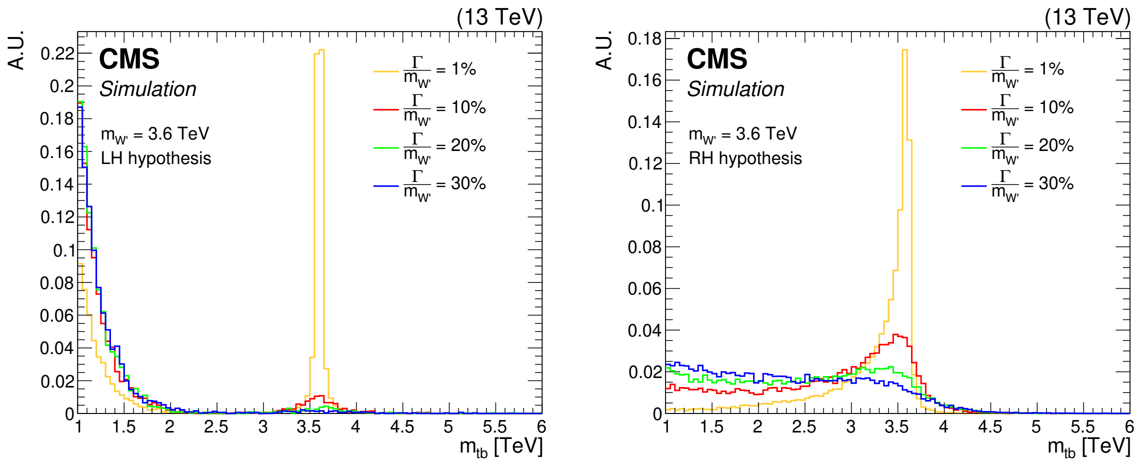

Figure 2: Representative distributions of the invariant mass of the top-bottom quark pair, m_{tb}, as originating from the W′ boson for left- (left) and right-handed (right) W′ bosons, with relative widths $\Gamma/m_{\mathrm{W}'}$ of 1, 10, 20, and 30% for a W′ boson mass of 3.6 TeV. For the LH, the signal is simulated including the SM production of single top quarks in the *s*-channel to correctly take into account the relative interference with the production of the W′ boson.

This article is organized as follows: Section 2 gives a brief description of the CMS apparatus, Sections 3 and 4 report details on the data set and simulated samples, respectively, used in the analysis. Section 5 describes the requirements for the selection of events, while Sections 6 and 7 report the strategy for the reconstruction and the categorization of the events selected for analysis. The procedure for the prediction of most important backgrounds is described in Section 8, the systematic uncertainties affecting the analysis are reported in Section 9, and the limit extraction and results are detailed in Section 10. Tabulated results are provided in the HEPData record for this analysis [28].

2 The CMS detector

The central feature of the CMS apparatus is a superconducting solenoid of 6 m internal diameter, providing a magnetic field of 3.8 T. Within the solenoid volume are a silicon pixel and silicon strip tracker, a lead tungstate crystal electromagnetic calorimeter (ECAL), and a brass-and-scintillator hadron calorimeter (HCAL), each composed of a barrel and two endcap sections. Forward calorimeters extend the coverage in pseudorapidity (η) provided by the barrel and endcap detectors. Muons are detected in gas-ionization chambers embedded in the steel flux-return yoke outside the solenoid. A more detailed description of the CMS detector, together with a definition of the coordinate system used and the relevant kinematic variables, can be found in Ref. [29].

Events of interest are selected using a two-tiered trigger system [30]. The first level (L1), composed of custom hardware processors, uses information from the calorimeters and muon detectors to select events at a rate of around 100 kHz. The second level, known as the high-level trigger (HLT), consists of a farm of processors running a version of the full event reconstruction software optimized for fast processing that reduces the event rate to around 1 kHz before data storage.

3 Data samples and trigger requirements

This search uses proton-proton (pp) collision data at a center-of-mass energy $\sqrt{s} = 13$ TeV collected by the CMS experiment in the years 2016-2018, corresponding to an integrated luminosity of 138 fb^{-1}. Events that have passed a L1 trigger requirement for the presence of a muon, electron, photon, or jet are selected. The HLT selection requires an event to satisfy at least one of the following criteria:

- a muon is present without isolation requirements and with a transverse momentum $p_T > 50(100)$ GeV for 2016-2018 (2017-2018) data;
- an electron is present with isolation requirements on the hadronic energy and with $p_T > 27(35)$ GeV for 2016 (2017-2018) data;
- an electron is present without isolation requirements and with $p_T > 115$ GeV;
- a photon is present with $p_T > 175(200)$ GeV for 2016 (2017-2018) data;
- the p_T sum of all reconstructed jets is larger than $900(1050)$ GeV for 2016 (2017-2018) data.

Different trigger thresholds are used because of changes in instantaneous luminosity and detector configuration during the different data-taking periods. The inclusion of the photon trigger improves the trigger efficiency for electrons with very large p_T. The inclusion of the jet triggers improves the efficiency for selecting signal events by approximately 8% with respect to using lepton triggers alone. Trigger efficiencies are derived for data and simulation in an event sample using orthogonal triggers requiring two different-flavor leptons, i.e., muon or electron pairs, and enriched in leptonically decaying top quark-antiquark pairs ($t\bar{t}$). Scale factors resulting from the differences between data and simulation are derived as functions of the $|\eta|$ and p_T of the lepton and applied as a correction to simulated events.

During the 2016-2017 data taking, a gradual shift in the timing of the inputs of the ECAL L1 trigger in the region $|\eta| > 2.0$ caused a specific trigger inefficiency ("ECAL Prefiring"). Dedicated scale factors are applied to simulation in order to account for this effect.

4 Simulated samples and signal modeling

Simulated background samples are generated at LO with MADGRAPH5_aMC@NLO [31] for the production of a W boson in association with jets (W + jets), and for events with jets arising exclusively from quantum chromodynamics (QCD) interactions (multijet events). For all these processes, the MADGRAPH5_aMC@NLO version 2.2.2 (2.4.2) is used for simulated events in conditions corresponding to the 2016 (2017-2018) data taking. The next-to-LO (NLO) generator POWHEG 2.0 [32–34] is used to simulate $t\bar{t}$ produced in association with jets [35] and single top quark [36] events.

The POWHEG 2.0 and MADGRAPH5_aMC@NLO generators are interfaced with PYTHIA with the following versions and underlying event tunes: version 8.226 and tune CUETP8M1 [37] for the simulated events used with 2016 data, and version 8.230 and tune CP5 [38] for those used with 2017-2018 data. The underlying event tune CUETP8M2T4 [39] is employed for the simulated $t\bar{t}$ events used with 2016 data, and the PYTHIA version 8.240 is adopted for simulated $t\bar{t}$ events used for 2017-2018 data. The background processes are initially normalized to their theoretical cross sections, using the highest order calculations available. The cross section for the $t\bar{t}$ background is computed at next-to-NLO (NNLO) accuracy in perturbative QCD using a soft-gluon resummation at next-to-next-to-leading logarithmic accuracy with the TOP++ 2.0 program [40]. For single top quark production, the NLO cross section as calculated with HATHOR 2.1 [41] is used. The W + jets cross section is calculated at LO and corrected with an inclusive k-factor to account for NLO in electroweak and NNLO in QCD corrections [42].

Signal event samples are generated at LO using MADGRAPH5_aMC@NLO version 2.4.2 interfaced to PYTHIA 8.230. The interactions of the W′ boson with the SM particles is described by the Lagrangian term:

$$\mathcal{L}^{\text{eff}} = \frac{V_{f_i f_j}}{2\sqrt{2}} g_{W'} \bar{f}_i \gamma_\mu [\alpha_R^{f_i f_j}(1+\gamma^5) + \alpha_L^{f_i f_j}(1-\gamma^5)] W'^\mu f_j + \text{h.c.}, \quad (1)$$

where $V_{f_i f_j}$ is the analogue of the Cabibbo–Kobayashi–Maskawa matrix if f_i and f_j represent quarks, while for leptons $V_{f_i f_j}$ is the identity matrix, and $g_{W'}$ is the coupling strength of the W′ boson. The parameters $\alpha_R^{f_i f_j}$ and $\alpha_L^{f_i f_j}$ regulate the coupling strengths to the two chiral fermion components, and depend on the specific gauge model represented in the new physics scenario.

In the following, all $\alpha_{L(R)}^{f_i f_j}$ are varied simultaneously, and we denote them simply as $\alpha_{L(R)}$. Samples corresponding to three chirality hypotheses have been generated: RH, with $\alpha_R = 1, \alpha_L = 0$, LH, with $\alpha_R = 0, \alpha_L = 1$, or mixed (LR), which consist of equal parts of LH and RH components, specifically $\alpha_R = \alpha_L = 1/\sqrt{2}$. The generated W′ mass in the samples ranges from 2 to 6 TeV. Narrow-width samples are generated with a width, Γ, set to 1% of the resonance mass $m_{W'}$ in mass steps of 0.2 TeV. Large-width samples are generated with Γ set to 10, 20, and 30% of $m_{W'}$, in mass steps of 0.8 TeV. All possible final states after top quark decays have been considered for the signal process. The signal cross sections are calculated with the MADGRAPH5_aMC@NLO generator.

Predictions for intermediate values of α_R and α_L are obtained by a procedure described in Ref. [43]. For an arbitrary combination of α_R and α_L, signal distributions, yields, and cross sections are obtained as a linear combination of the ones from LH, RH, and LR W′ samples, and the SM single top s-channel sample. Values of α_R and α_L between 0 and 1 are considered in steps of 0.1.

The default parametrization of the PDFs used in all simulations is NNPDF3.0 [44] or NNPDF3.1 [45] at LO or NLO QCD, with the order matching that of the matrix element calculation. All generated events undergo a full simulation of the detector response according to the model of the CMS detector within GEANT4 [46]. All simulated samples include additional pp interaction in the same or nearby bunch crossings (pileup) and are weighted such that the distribution of the number of interactions in each event agrees with that observed in the data.

5 Physics object reconstruction and selection

The decay chain considered for this analysis is $W' \to tb \to \ell\nu bb$. Its expected experimental signature consists of one muon or electron, the hadronization products of the two b quarks (b jets), and one neutrino escaping the detector without generating a signal, causing a momentum imbalance in the total p_T of the reconstructed events. The experimental signature sought for therefore includes one reconstructed electron or muon, a large amount of missing momentum to the kinematic closure of the events, and at least two jets. The main backgrounds that mimic this signature are $t\bar{t}$ and single top quark processes where a top quark decays through a leptonic decay chain, W + jets production where the W boson decays into a lepton and a neutrino, and QCD multijet processes where a fake or nonprompt lepton is reconstructed as a prompt lepton.

After the trigger selection, an offline reconstruction of the events is performed to identify decay vertices and particle candidates. Particle candidates in the event are reconstructed using the particle-flow (PF) algorithm [47], which performs a global event reconstruction by combining the information from the various elements of the CMS detector, and which provides the identification of muons, electrons, photons, and charged and neutral hadrons.

The primary vertex is taken to be the vertex corresponding to the hardest scattering in the event, evaluated using tracking information alone, as described in Section 9.4.1 of Ref. [48]. The physics objects considered are the jets formed by clustering the tracks from the candidate vertex by the jet-finding algorithm [49, 50] and the missing p_T ($\vec{p}_T^{\,miss}$) associated with the vertex, taken as the negative vector p_T sum of the jets. The primary vertex must be within 24 cm of the nominal interaction point along the beam axis and within 2 cm in the transverse plane.

Muons considered for this analysis must have $p_T > 55$ GeV, and be within the acceptance of the muon system, $|\eta| < 2.4$. Electrons considered for this analysis must have $p_T > 50$ GeV, be within an $|\eta| < 2.2$, and pass a multivariate analysis based identification criterion that has an efficiency of 90% for prompt electrons, i.e., electrons coming from a hard-scattering process, as opposed to nonprompt ones from a hadron decay chain. Electrons in the barrel-endcap gap at $1.444 < |\eta| < 1.566$ are excluded from the selection, because the reconstruction of an electron object in this region is not optimal. In order to distinguish between prompt leptons and the ones coming from hadronic decay chains, isolation criteria are applied based on the deposited energy sum of hadrons and photons in a cone around the lepton direction, compared to the lepton momentum. For this analysis, an optimized version of the "mini-isolation" variable originally suggested in Ref. [51] is adopted, tailored for cases where the lepton is produced in a boosted top quark decay. Leptons in signal events often fall within the radius of the jet produced by the b quark arising from the top quark decay, and the separation in the η–ϕ plane between the lepton and the jet axis decreases with the increasing Lorentz boost of the top quark. In order to recover efficiency compared to standard fixed-radius isolation criteria, the variable

I_{mini} is defined as the ratio between $S_I(R)$ and p_T^ℓ:

$$I_{\text{mini}} = \frac{S_I(R)}{p_T^\ell}, \text{with } R = \frac{10\,\text{GeV}}{\min(\max(p_T^\ell, 50\,\text{GeV}), 200\,\text{GeV})}, \quad (2)$$

where $S_I(R)$ is the scalar p_T sum of charged- and neutral-hadrons, and photon PF candidates inside a cone with a variable radius R around the lepton in the η–ϕ plane and p_T^ℓ is the p_T of the lepton. The isolation variable I_{mini} is calculated for each lepton, where the cone size decreases with increasing p_T^ℓ as indicated in Eq. (2), reducing the probability of the overlap with a jet for boosted topologies. For this analysis, muons and electrons are required to have a mini isolation $I_{\text{mini}} < 0.1$. Events are considered for further analysis if they contain exactly one electron or muon satisfying the requirements listed above.

In order to reduce the background contribution, particularly from dileptonic $t\bar{t}$ events, events with at least one additional muon with $p_T > 35\,\text{GeV}$, $|\eta| < 2.4$, and $I_{\text{mini}} < 0.4$ or at least one additional electron with $p_T > 35\,\text{GeV}$, $|\eta| < 2.2$, and $I_{\text{mini}} < 0.4$ are discarded.

Scale factors accounting for the differences between the lepton identification and mini-isolation efficiencies in data and simulation are derived using a $Z \to \ell\ell$ sample, as functions of the $|\eta|$ and p_T of the lepton, and applied as corrections to simulated events.

Jets are reconstructed with the anti-k_T algorithm [49] as implemented in the FASTJET package [50]. Two types of jet definitions are used in the analysis:

- jets clustered with a radius parameter of $R = 0.4$ (AK4 jets) are considered for top quark and W′ boson candidate reconstruction;
- jets clustered with a radius parameter of $R = 0.8$ (AK8 jets) are also used in the analysis, first to perform a loose selection, and then in the event categorization to veto hadronic top quark decays coming from SM backgrounds.

The anti-k_T algorithms are both ran onto the same set of particle candidates reconstructed by the PF algorithm, and the two resulting collections of jets are not mutually exclusive. The hadronization products of a single quark can therefore be clustered both in an AK4 and in an AK8 jet in the same event.

For the AK8 jets, the "modified mass drop tagger" algorithm [52, 53], also known as the "soft drop" (SD) algorithm, with angular exponent $\beta = 0$, soft cutoff threshold $z_{\text{cut}} < 0.1$, and characteristic radius $R_0 = 0.8$ [54], is applied to remove soft, wide-angle radiation from the jet.

The charged hadron subtraction algorithm [55] is applied to the AK4 jets to remove charged hadrons not originating from the primary vertex, while for the AK8 jets the pileup-per-particle identification algorithm [56] is employed, which assigns a weight to each charged or neutral PF candidate according to the likelihood that the candidate originates from a pileup interaction. The weight is then used to rescale the particle four-momentum. Correction factors as functions of the p_T, η, energy density, and the area of the jet are applied to calibrate the jet energy scale. The jet energy resolution for simulated jets is adjusted to reproduce the resolution observed in data [57]. Jets potentially coming from instrumental or reconstruction issues are discarded with dedicated selection criteria [58].

The AK4 jets with $|\eta| < 2.4$ and $p_T > 100\,\text{GeV}$ are included in the analysis, and it is required that at least two of them are present with $p_T > 300$ and $150\,\text{GeV}$ for the leading and subleading jets, respectively. The presence of at least two AK8 jets with $|\eta| < 2.4$ and $p_T > 170\,\text{GeV}$ is also required to reduce contamination from low-energy $t\bar{t}$ and QCD events, and at the same time allows for the application of a further selection requirement donwstreams in the analysis, described in detail in Section 7.

A deep neural network based tagger, DeepJet [59–61], is used to identify AK4 jets stemming from the hadronization of b quarks, utilizing information from the tracks, neutral particles, and the secondary vertices within the jet. The thresholds used for the DeepJet b tagger in this analysis correspond to a mistag probability for jets initiated by light quarks or gluons with $p_{\mathrm{T}} > 500\,\mathrm{GeV}$ of approximately 5% in 2016 and 1% in 2017-2018. The b tagging performance is better in 2017-2018 than in 2016 because of the upgrade of the pixel detector of the CMS tracker in 2017. This choice of thresholds provides an efficiency of approximately 75% (60%) at $p_{\mathrm{T}} = 500\,\mathrm{GeV}$ and 65% (50%) at $p_{\mathrm{T}} = 1000\,\mathrm{GeV}$ for jets initiated by b quarks in the HCAL barrel (endcap) region. To match the shape of the DeepJet discriminator in data and simulation, corrections as functions of the p_{T} and η of AK4 jets, derived using samples enriched in dileptonic $\mathrm{t\bar{t}}$ events for jets initiated by b and c quarks, and Z+jets events for the jets initiated by light quarks and gluons, are applied in simulation.

The PF-based $\vec{p}_{\mathrm{T}}^{\,\mathrm{miss}}$, is the negative vectorial p_{T} sum of the identified PF particles, and its magnitude is referred to as $p_{\mathrm{T}}^{\mathrm{miss}}$. The signal processes are expected to have a significant amount of $p_{\mathrm{T}}^{\mathrm{miss}}$. A requirement that an event has $p_{\mathrm{T}}^{\mathrm{miss}} > 120\,\mathrm{GeV}$ reduces the contamination from QCD background processes, which mainly comes from $\mathrm{b\bar{b}}$ and $\mathrm{c\bar{c}}$ production, where the $p_{\mathrm{T}}^{\mathrm{miss}}$ originates from nonprompt neutrinos and resolution effects and is thus typically of smaller magnitude.

6 Top quark and W′ boson reconstruction

For events passing the selection defined in Section 5, a kinematic reconstruction of top quark candidates from the W′ boson decay is performed. The top quark four-momentum is reconstructed starting from the selected lepton, the $\vec{p}_{\mathrm{T}}^{\,\mathrm{miss}}$, and one of the AK4 jets considered in the event.

The top quark momentum is reconstructed according to the algorithm described in Ref. [62]. The reconstruction consists of the following steps:

- the $\vec{p}_{\mathrm{T}}^{\,\mathrm{miss}}$ is taken as the transverse component of the neutrino momentum, $\vec{p}_{\mathrm{T}}^{\,\nu}$;
- the longitudinal component of the neutrino momentum, p_z^{ν}, is calculated imposing the mass of the lepton-neutrino pair is equal to the W boson mass [63]. The masses of the lepton and the neutrino are taken to be zero, resulting in a second order equation for p_z^{ν}. An additional step is needed if the equation admits two real solutions or two imaginary solutions;
- if two real solutions are found, the one that results in a value of the W boson mass closest to the world average value is chosen. Since the reconstructed leptons have a very small, but nonzero mass, the resulting reconstructed W boson mass will not be equal to the imposed SM value;
- if two imaginary solutions are found, the constraint $\vec{p}_{\mathrm{T}}^{\,\nu} = \vec{p}_{\mathrm{T}}^{\,\mathrm{miss}}$ is released. This allows the discriminant of the second-order equation to be set to zero, finding a single solution for p_z^{ν}, and one constraint on the transverse components of the neutrino. To fully determine the neutrino p_{T}, an additional condition is set by minimizing the vectorial distance between $\vec{p}_{\mathrm{T}}^{\,\nu}$ and $\vec{p}_{\mathrm{T}}^{\,\mathrm{miss}}$.

Given that there are at least two AK4 jets in each event, multiple top quark candidates can be constructed. It is therefore necessary to define a criterion to choose the jet assigned to the top quark, henceforth referred to as $\mathrm{j_t}$.

Taking into account the kinematic features of the decay chain, the following three criteria are considered in performing the jet assignment:

- **mass criterion**: since the W boson and the candidate jet are products of the top quark decay, one expects the invariant mass of the sum of the corresponding four-momenta to be close to the world-average value of the top quark mass [63]. For the mass criterion we therefore choose, as j_t, the one that results in a reconstructed top quark mass (M_t) closest to the nominal value.
- **closest criterion**: we choose, as j_t, the jet with the lowest angular separation ΔR from the lepton in the event.
- **subleading criterion**: one expects the highest p_T AK4 jet (the "leading jet") to arise from the b quark coming directly from the W′ boson decay, while the second jet in p_T (the "subleading jet") should originate from the b quark coming from the t quark decay. This criterion therefore chooses the subleading jet for the reconstruction of the t quark.

If the same AK4 jet satisfies at least two of these criteria, it is chosen as j_t and the top quark four momentum is reconstructed. If three different AK4 jets are selected by the three criteria, the one passing the mass criterion is selected.

In order to reconstruct the W′ boson candidate in the event, another AK4 jet is needed, referred to as $j_{W'}$. This AK4 jet is chosen as the one with the highest p_T among the jets not chosen as the j_t.

If there are fewer than two b-tagged jets, the j_t and $j_{W'}$ selection procedure described above is applied to the entire jet collection. If there are at least two b-tagged jets, the j_t and $j_{W'}$ selection procedure is applied only to the b jet collection.

The reconstructed $m_{W'}$, $M_{\ell\nu jj}$, with $\ell = \mu, e$, is obtained as the invariant mass of the reconstructed top quark and $j_{W'}$ four-momenta. The quality of the reconstruction algorithm is evaluated on a simulated signal sample with an $m_{W'}$ of 4 TeV, and it is assessed that the correct jet is assigned in 91% of the cases for the top quark, and in 87% of the cases for the W′ boson.

7 Event categorization

Events are divided into four regions, depending on the number of b tagged jets, and whether they are selected as j_t or $j_{W'}$. If an event has at least two b-tagged jets, it belongs to the R2B signal-enriched region. Conversely, if there are fewer than two b-tagged jets, the region is labeled as R0, a control and validation region with no signal contamination, if none of j_t and $j_{W'}$ are b-tagged jets, RT, a signal-enriched region, if only the j_t is b-tagged, and RW′, another signal-enriched region, if only the $j_{W'}$ is b-tagged. The four regions are described in Table 1.

After the event is assigned to one of the regions, events are further categorized in so-called subregions. Two variables are used in this step:

- the soft-drop mass $M_{SD,AK8}$ of the AK8 jet (j_{AK8}) with the smallest angular distance in the η–ϕ plane, $\Delta R(j_{W'}, j_{AK8})$, to the $j_{W'}$. If $\Delta R(j_{W'}, j_{AK8}) < 0.4$, the soft-drop mass of this j_{AK8} is taken to be $M_{SD,AK8}$. If $\Delta R(j_{W'}, j_{AK8}) > 0.4$, the event is not retained for further analysis.
- the reconstructed top quark mass M_t, defined as the invariant mass of the reconstructed top quark four-momentum vector, obtained with the procedure described in in Section 6.

Table 1: The regions defined in the analysis depending on the number of b-tagged jets and of the j_t and $j_{W'}$ assignment.

Number of b jets	j_t is a b-tagged jet	$j_{W'}$ is a b-tagged jet	Type of category (label)
0	no	no	Control region (R0)
	Signal-enriched regions		
1	yes	no	t jet region (RT)
1	no	yes	W′ jet region (RW′)
≥2	yes	yes	Region with 2 b jets (R2B)

For each of the regions of Table 1, four subregions are identified and labeled using subscripts A, B, C, and D, as defined below, and illustrated in Fig. 3:

- subregion A requires $M_{SD,AK8} < 60\,GeV$ and $120 < M_t < 220\,GeV$;
- subregion B requires $M_{SD,AK8} < 60\,GeV$, $M_t > 220\,GeV$, in R0, RW′, and RT, and $M_{SD,AK8} < 30\,GeV$, $M_t > 340\,GeV$ for R2B. This different selection in R2B prevents signal contamination;
- subregion C requires $M_{SD,AK8} > 60\,GeV$ and $120 < M_t < 220\,GeV$;
- subregion D requires $M_{SD,AK8} > 60\,GeV$ and $M_t < 120$ or $M_t > 220\,GeV$.

The subregions $R2B_A$, RT_A, and RW'_A are used for signal extraction. In such subregions, the requirement on $M_{SD,AK8}$ reduces contamination from $t\bar{t}$ events decaying into a $\ell +$ jets final state, where the j_t likely comes from a genuine leptonically-decaying top quark, and the $j_{W'}$ is likely to come from a hadronically decaying top quark. For hadronically decaying, highly energetic top quarks, the decay products are often reconstructed as a single AK8 jet whose soft-drop mass is close to the top quark mass. For the same subregions, the requirement on M_t reduces contamination from W + jets and multijet QCD events, where a genuine leptonically-decaying top quark is not present in the event, as well as from top quark candidates from $t\bar{t}$ events in the $\ell +$ jets channel where the b jet association failed, or from residual dilepton events that happened to pass the lepton veto.

The subregions $R0_A$ and RW'_A are dominated by W + jets events, while RT_A and $R2B_A$ are dominated by $t\bar{t}$ events, with some contributions from W + jets, single top quark, and multijet QCD events.

The subregion $R0_A$ is not suitable for signal extraction because of the abundance of W + jets events, with jets coming from light quarks or gluons. For this reason, this subregion is used instead for validation of the background extraction procedure defined below.

Regions B are utilized to determine the overall shape and normalization of the different backgrounds, and Regions C and D to assess, and constraint, systematic uncertainties.

8 Background estimation

The modeling of $t\bar{t}$, W + jets, and single top quark production, especially at very high values of $M_{\ell\nu jj}$, is sensitive to higher-order QCD and electroweak corrections that are not included in simulations. In order to correct for these effects, the overall distribution of the background is extracted from the data. The strategy followed in this paper consists in deriving from the entire 2016-2018 data set a single distribution for all the three major background contributions, $t\bar{t}$, W + jets, and single top quark production. The multijet QCD process is instead a minor background and simulation is used for its prediction. The background contamination procedure is described in detail in this section while a schematic view is shown in Fig. 3.

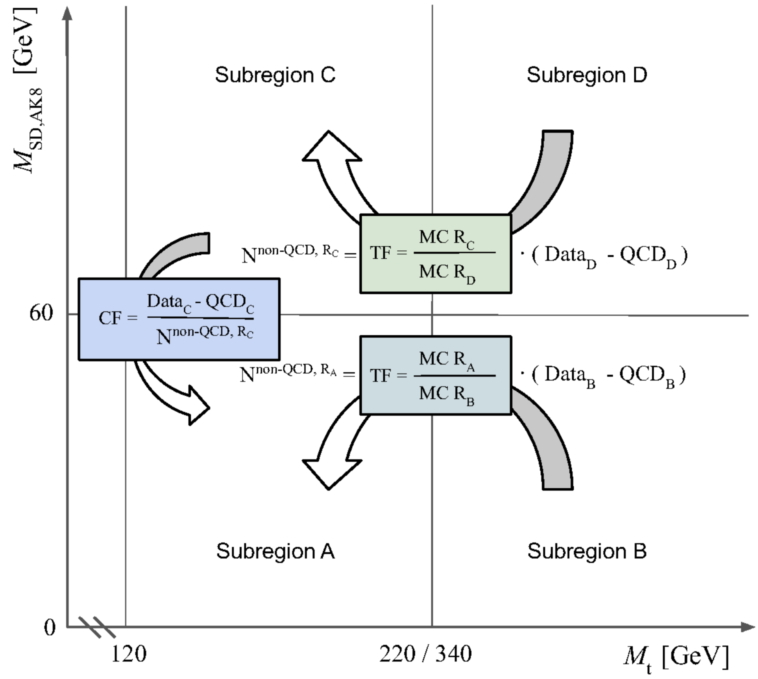

Figure 3: A visual representation of the subregions and their usage in the background extraction procedure. The x axis reports the requirements applied on M_{t} in order to define the subregions while the y axis represents the soft-drop mass of the AK8 jet associated to the AK4 jet used to reconstruct the W′ boson ($M_{\mathrm{SD,AK8}}$).

For each of the three subregions enriched with signal, $\mathrm{R2B_A}$, $\mathrm{RT_A}$, and $\mathrm{RW'_A}$, as well as the subregion $\mathrm{R0_A}$, all indicated henceforth as "fit subregions", the corresponding subregion B is used in order to determine the overall shape and normalization of the reconstructed $M_{\ell\nu\mathrm{jj}}$ distribution for the background processes. Simulations are used to determine a transfer function, $TF(M_{\ell\nu\mathrm{jj}})$, from each of those subregions to the corresponding signal-enriched subregion. In the following we describe the procedure in detail, denoting as $\mathrm{R_A}$, $\mathrm{R_B}$, $\mathrm{R_C}$, and $\mathrm{R_D}$ the fit subregion A and the corresponding subregions B, C, and D, respectively, where R can be either R2B, RT, RW′, or R0.

The $M_{\ell\nu\mathrm{jj}}$ distribution for the sum of the non-QCD simulated background components is considered in $\mathrm{R_A}$ and in $\mathrm{R_B}$. The ratio of the two distributions is then modeled with a transfer function that takes the form of:

$$TF(M_{\ell\nu\mathrm{jj}}) = a\mathrm{e}^{bM_{\ell\nu\mathrm{jj}}} + cM_{\ell\nu\mathrm{jj}} + d, \quad (3)$$

with a, b, c, d being parameters extracted from a maximum likelihood fit to the Monte Carlo (MC) simulation for non-QCD backgrounds. The following steps are then performed for each bin of the $M_{\ell\nu\mathrm{jj}}$ distribution.

A fit to the $M_{\ell\nu\mathrm{jj}}$ distribution in data is performed in the subregion $\mathrm{R_B}$ with the same functional form as in Eq. (3) with parameters extracted from a maximum likelihood fit. The number of events in each bin as estimated by the fit is then used. The QCD multijet contribution in R_B is estimated from simulation and subtracted from the resulting distribution. The distribution is then multiplied by the binned transfer function TF from Eq. (3) resulting in the background prediction for non-QCD events in the subregion R_A. The overall procedure can be summarized as:

$$N^{\text{non-QCD}, R_A} = \text{TF} \cdot (N^{\text{Data}\, R_B} - N^{\text{QCD, MC}\, R_B}), \tag{4}$$

where $N^{\text{non-QCD}, R_A}$ is the predicted number of events in the signal subregion R_A, $N^{\text{Data}\, R_B}$ is the number of events estimated from the fit to data in R_B, and $N^{\text{QCD, MC}\, R_B}$ is the number of QCD multijet events predicted by simulation in R_B.

Subregions R_C and R_D are used to assess potential systematic influences on the procedure, either due to the kinematic difference of the $M_{\ell\nu jj}$ spectra induced by the selection on M_t and not accounted for in simulations, or to the different background composition in the two subregions. The background extraction is repeated in R_C and R_D, by modeling the $M_{\ell\nu jj}$ distribution in data in R_D with a function of the same form as in Eq. (3). A transfer function $TF(M_{\ell\nu jj})_{CD}$ between R_C and R_D is derived from simulation and modeled with a function of the same form as in Eq. (3). The number of events in R_C is obtained as:

$$N^{\text{non-QCD}, R_C} = \text{TF}_{CD} \cdot (N^{\text{Data}\, R_D} - N^{\text{QCD, MC}\, R_D}). \tag{5}$$

A bin-by-bin correction factor CF is then defined as:

$$\text{CF} = \frac{N^{\text{non-QCD, Data}\, R_C}}{N^{\text{non-QCD}, R_C}}, \tag{6}$$

where $N^{\text{non-QCD, Data}\, R_C}$ is the number of events in data in R_C, obtained after subtracting the QCD events in R_C, as determined from simulation.

An alternative shape to the prediction in Eq. (4) is obtained as follows:

$$N^{\text{non-QCD, corr}\, R_A} = \text{CF} \cdot N^{\text{non-QCD}, R_A}. \tag{7}$$

The full bin-by-bin difference between the prediction obtained in Eq. (4) and the one in Eq. (7) is taken as the systematic uncertainty.

Summarizing the procedure, for each subregion the $TF(M_{\ell\nu jj})$ from R_B to R_A is obtained via a fit to simulation, then multiplied by the distribution in data, which is derived with a fit to R_B in order to soothe statistical effects. To this distribution a small bin-by-bin correction factor is applied as a systematic uncertainty, obtained by repeating the same procedure in R_C and d, in order to account for potential biases in the method.

9 Systematic uncertainties

Several sources of systematic uncertainties have been taken into account. All uncertainties that can be applied to background processes are propagated through the background estimation procedure.

- Luminosity: an uncertainty of 1.6% in the integrated luminosity is used [64–66]. This uncertainty is treated as affecting only the number of events, and as correlated across processes and muon and electron channels.
- Parton distribution functions: the uncertainty due to the PDFs is estimated using reweighted distributions derived from all PDF sets of NNPDF3.1 or NNPDF3.0 according to the PDF4LHC recommendations [67].
- Factorization and renormalization scales: uncertainties related to the choice of these two scales are obtained by considering all variations obtained by setting alternative scales to double or half of the nominal value. The maximum over all variations is taken as the uncertainty. These uncertainties are calculated independently for each process.
- Multijet QCD background: a rate uncertainty corresponding to 50% of the nominal cross section is considered as the uncertainty in the number of QCD multijet events.
- b tagging and mistagging efficiency: scale factors are applied to simulated events, allowing the reproduction of the b-tagging and mistagging efficiencies, as measured in data. The uncertainty from the scale-factor measurement is propagated to obtain the systematic uncertainty.
- Pileup modeling: systematic uncertainties related to pileup modeling are taken into account by varying the total inelastic pp cross section of 69.2 mb by $\pm$4.6% [68].
- Trigger efficiency: data-to-simulation scale factors have been measured in a control sample selected with different trigger requirements with respect to the ones applied for this analysis, selecting a statistically independent event sample. The systematic uncertainty due to the trigger efficiency is obtained by shifting the values of the trigger scale factors up and down by their uncertainties.
- ECAL prefiring corrections: in 2016-2017, a small fraction of ECAL trigger primitives was associated with a wrong bunch crossing. Events have been corrected for this effect with a per-event weight, and the corresponding uncertainties have been propagated to the signal yield.
- Jet energy scale and resolution: in simulated events all reconstructed jet four-momenta are simultaneously varied according to the η- and p_{T}-dependent uncertainties in the jet energy scale. In order to evaluate the systematic effect due to differences in the jet energy resolution between data and simulation, a smearing is also applied to simulated events by increasing or decreasing the jet resolutions by their uncertainties [57]. These variations in jet four-momenta are also propagated to the $\vec{p}_{\mathrm{T}}^{\mathrm{miss}}$.
- Background modeling, statistical uncertainties: as described in Section 8, fits are performed to determine the background shape in the $\mathrm{R_B}$ and to obtain the $TF(M_{\ell\nu\mathrm{jj}})$. Statistical uncertainties are propagated to the final distributions. The uncertainties in the parameters obtained from the two fits, to the $TF(M_{\ell\nu\mathrm{jj}})$ and to the $M_{\ell\nu\mathrm{jj}}$ distribution, are propagated to the predicted number of events in each bin. These uncertainties are treated as uncorrelated across all categories and lepton channels.
- Background modeling, alternative shapes: alternative models with respect to the form described in Eq. 3 and Sec. 8 are considered for the function used to model the data in $\mathrm{R_B}$ and for the function used to model the $TF(M_{\ell\nu\mathrm{jj}})$. In this specific scenario, the fit for deriving the number of events starts from 1.5 TeV instead of the nominal starting point of 1 TeV. The fit function is applied within this range to determine the number of events. The resulting uncertainty is initially asymmetric, as it considers the difference between the fit distribution and the nominal distribution. To obtain a

two-sided (symmetric) variation, the full difference between the fit distribution and the nominal distribution is considered, but with opposite signs.

- Background modeling, alternative model: an alternative function is considered for the function used to model the data: the data are described with a Landau function without any further change in the procedure. This uncertainty is obtained by considering the full difference with the nominal distribution and symmetrized to get a two-sided variation.
- Background composition: when obtaining the $TF(M_{\ell\nu jj})$, the dependence on the background composition of $t\bar{t}$, $W+$jets, and single top quark production is taken into account by varying each of them independently by a relative factor of $\pm 80\%$ of the expected yield. The entire procedure is repeated by varying each background in all subregions, deriving a new $TF(M_{\ell\nu jj})$ between R_A and R_B, and applying the $TF(M_{\ell\nu jj})$ to the R_B distribution from data. Different alternative templates are obtained with this procedure for each background. This is done in order to reduce the dependence of the fit on events in the low part of the $M_{\ell\nu jj}$ spectrum, and to separate the low-mass regime from the high-mass regime in the background. This uncertainty is designed to cover differences in the relative fraction of backgrounds among regions, statistical fluctuations in simulation, and the process cross section in the very high-energy regime.
- Background rate: in order to disentangle the rate and shape effects of the background composition uncertainty, the total background yield for each subregion is left free to float in the fit.
- Background correction factors: an uncertainty in the correction factor is determined, by considering the full difference between the final distribution with and without the correction (cf. Eqs. (4) and (7)). This uncertainty is then symmetrized by considering the full difference, but with the opposite sign.
- Limited size of simulated samples: the statistical uncertainty due to the limited size of the simulated event samples is evaluated for each bin with the Barlow–Beeston "lite" method [69, 70].

The background modeling uncertainties are considered as uncorrelated among regions and lepton channels. This choice is motivated by kinematic and background composition differences among regions and lepton channels. Lepton identification and trigger uncertainties are considered as correlated among regions but as uncorrelated among lepton channels. Experimental uncertainties are considered as correlated among regions and lepton channels. Jet energy scale and resolution uncertainties are uncorrelated among years due to differences in detector conditions. Factorization and renormalization scale uncertainties are uncorrelated between all processes, while PDF uncertainties are correlated instead.

10 Statistical inference and results

A simultaneous maximum likelihood fit to data is performed using the distribution of $M_{\ell\nu jj}$ in both the muon and electron channels. All systematic uncertainties described in Section 9 are treated as nuisance parameters.

A first fit is performed in the subregion $R0_A$ in order to validate the background estimation procedure using a statistically independent sample. The post-fit distributions of the reconstructed $M_{\ell\nu jj}$ are shown in Fig. 4. The distributions are in agreement with the data, as can be seen in the lower panel, where the data minus the expected number of events are presented, normalized to the statistical uncertainty of the data. The orange band represents the systematic uncertainties, also normalized to the statistical uncertainty of the data. In addition, a goodness of fit test was conducted, yielding a p-value of 0.128 [71]. Signal injection tests were performed, ensuring that no significant bias is present due to the statistical inference procedure.

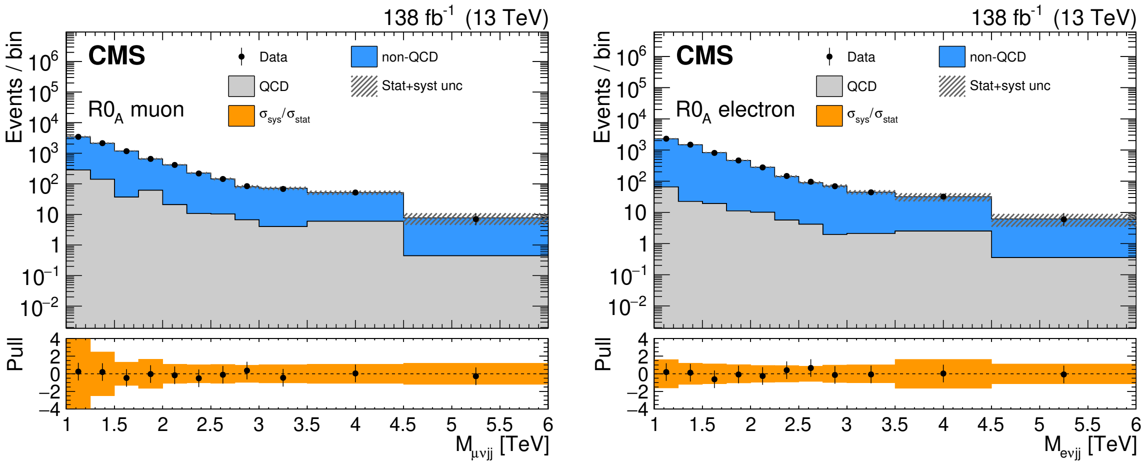

Figure 4: Post-fit distributions of $M_{\ell\nu jj}$ in the $R0_A$ control subregion for muons (left) or electrons (right). The lower panel reports the data minus the expected number of events normalized to the statistical uncertainty of the data. The orange band represents the systematic uncertainties, also normalized to the statistical uncertainty of the data.

To check for the presence of a possible signal in the data, the fit procedure is carried out simultaneously using the distributions of $M_{\ell\nu jj}$ in the three subregions $R2B_A$, RT_A, RW'_A of the muon and electron channels.

All signal hypotheses described in Section 1 are probed in separate fits, including purely left- and right-handed chiralities of the W′ boson, and width hypotheses of 1, 10, 20, and 30% of the $m_{W'}$ over a range between 2-6 TeV.

A local excess over the background is observed for masses $m_{W'}$ between 3.4-4.4 TeV, with a maximum local significance of 2.6 standard deviations at 3.8 TeV for a 1% relative width, and a right-handed signal hypothesis. The most significant contribution to the excess comes from the $R2B_A$ region for the muon channel, making it the most sensitive subregion in the analysis. An important contribution also comes from the $R2B_A$ in the electron channel and RT_A in the muon channel. The global significance of this excess is 2.0 standard deviations. The corresponding post-fit $M_{\ell\nu jj}$ distributions in the background plus signal hypothesis are shown in Fig. 5. Events in data corresponding to the excess region in $M_{\ell\nu jj}$ were scrutinized, by studying the features of reconstructed physics objects to ensure that all were correctly reconstructed.

The most important systematic uncertainties affecting the result are those related to the b tagging efficiency, the background composition, the background alternative shape, and the background correction factors.

Upper limits on the production cross section are extracted by following the CL_s prescription [72, 73], making use of the asymptotic approximation [74]. Cross section limits are derived for each value of the W′ mass, width, and chirality, and compared with the prediction obtained as described in Section 8. Figures 6 and 7 show, for LH and RH hypotheses respectively, the upper limits on the cross section as a function of $m_{W'}$ in the scenarios with $\Gamma/m_{W'}$ = 1, 10, 20, and 30%.

The observed 95% CL upper limits on the production cross section for a right- and left-handed W′ boson in the tb final state are shown in Fig. 8, as functions of $m_{W'}$ and relative width $\Gamma/m_{W'}$. Numbers in red represent values of the excluded cross sections lower than the theoretical ones for the analyzed model.

Models with values of the parameters α_R and α_L, which regulate the chirality fraction as defined in Eq. (1), ranging from 0.1 to 0.9 in steps of 0.1 were also tested in the hypothesis of $\Gamma/m_{W'} =$ 1%. Under the hypothesis of a narrow width, a simple formula can be used to obtain the cross section of the process from the ones for single top s-channel production (σ_{SM}), pure LH (σ_L), pure RH (σ_R), and the mixed LH and RH (σ_{LR}) case with $\alpha_R = \alpha_L$ [75]:

$$\sigma = (1-\alpha_L^2)\sigma_{SM} + \frac{1}{\alpha_L^2+\alpha_R^2}\left[\alpha_L^2(\alpha_L^2-\alpha_R^2)\sigma_L + \alpha_R^2(\alpha_R^2-\alpha_L^2)\sigma_R + 4\alpha_L^2\alpha_R^2\sigma_{LR} - 2\alpha_L^2\alpha_R^2\sigma_{SM}\right]. \quad (8)$$

Making use of this formula, we can evaluate upper limits on the production cross section, to allow for re-interpretation in a wide array of models, or on the W′ boson once the theoretical cross section is specified. The observed 95% CL upper limits on the production cross section for a generalized left-right coupling of the W′ boson to a t and a b quark are obtained for masses of the W′ boson between 2 and 6 TeV in steps of 0.8 TeV. The observed limits are reported in Fig. 9.

Limits on $m_{W'}$ are also obtained for all tested values of the generalized left-right coupling of the W′ boson to a t and a b quark. Figure 10 shows the expected and observed limits on $m_{W'}$.

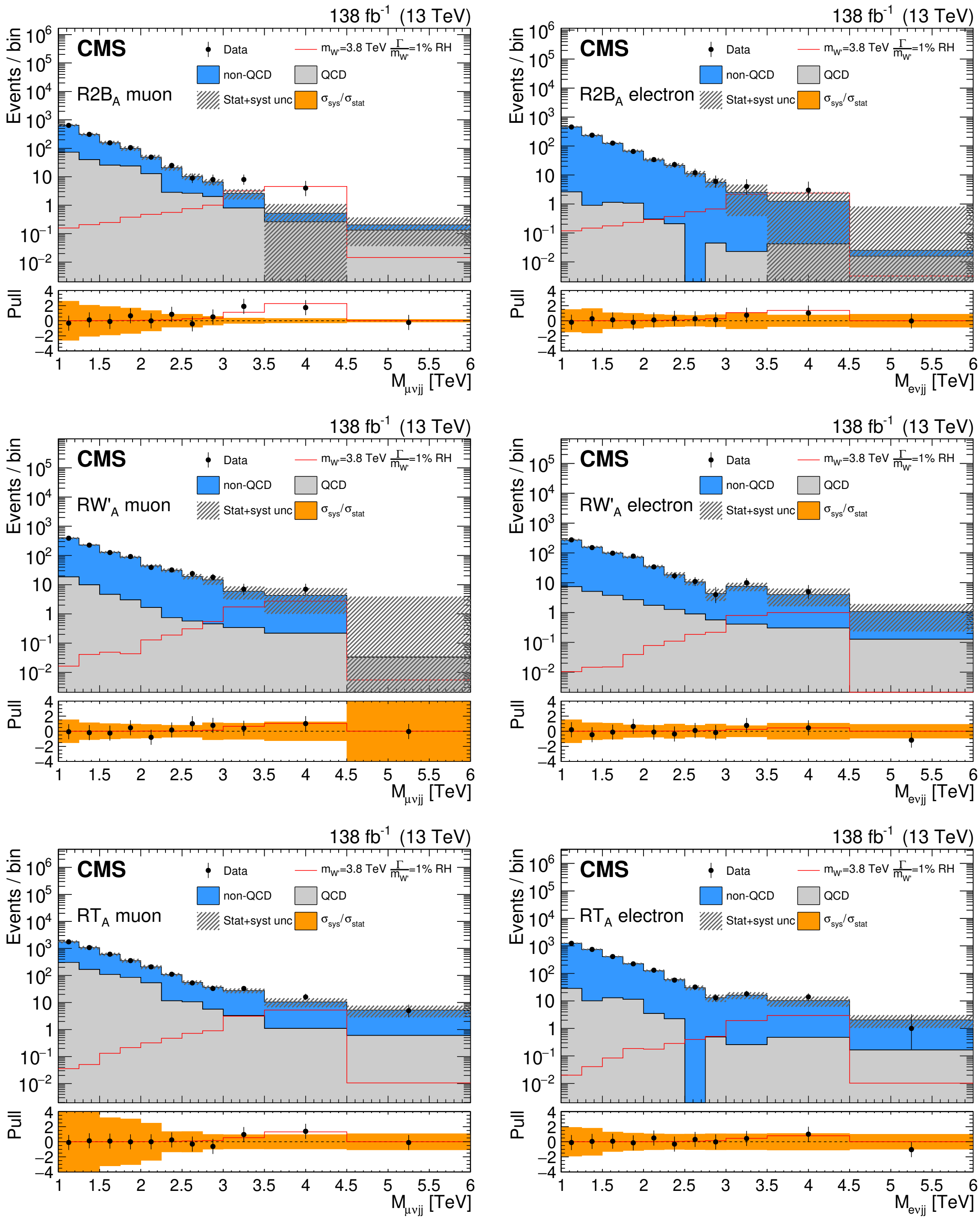

Figure 5: Post-fit distributions of $M_{\ell\nu jj}$ in the R2B$_A$ (upper), RW$'_A$ (middle), and RT$_A$ (lower) subregions for muons (left column) and electrons (right column). All process yields and nuisance parameters are set to the values obtained from the background plus signal fit. The signal considered for the fit corresponds to the purely right-handed production of a W$'$ with $m_{W'}$ of 3.6 TeV and a relative width of 1% of the $m_{W'}$, and is represented by the solid red line. The lower panels show the data minus the expected number of events, normalized to the statistical uncertainty of the data. The orange band represents the systematic uncertainties, also normalized to the statistical uncertainty of the data.

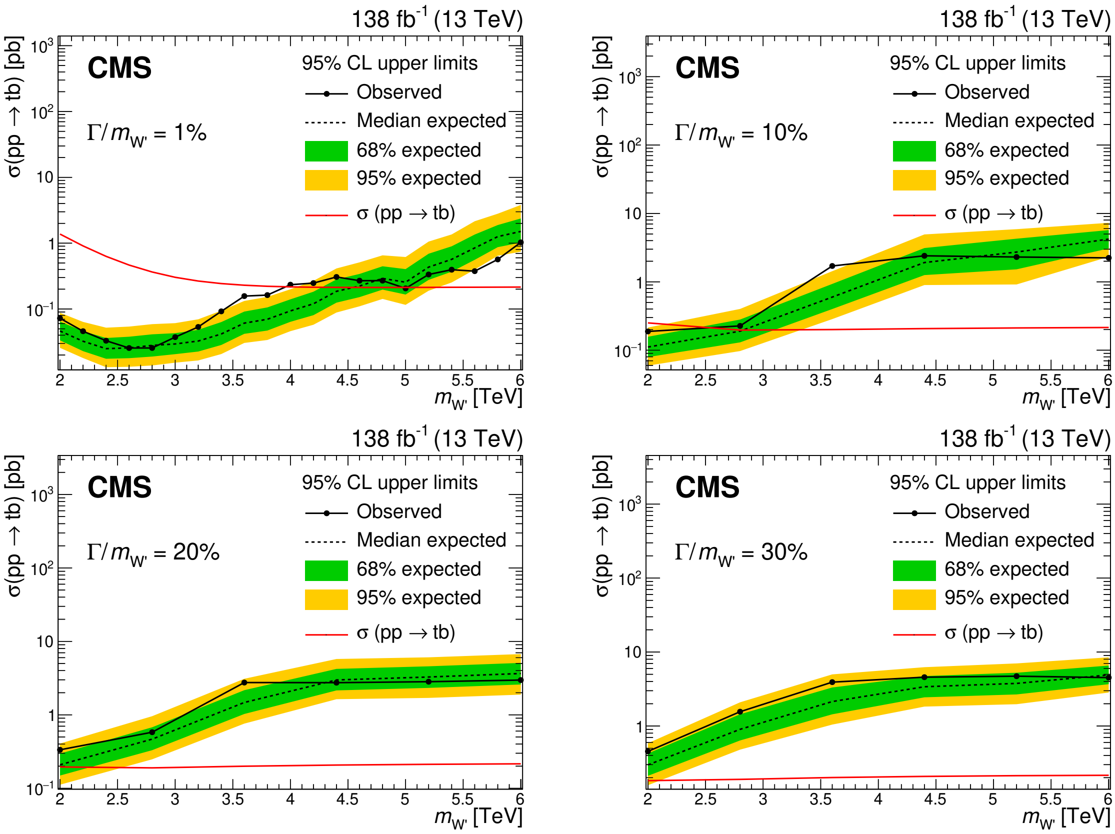

Figure 6: Observed and expected 95% CL upper limits on the product of the production cross section for production of a tb quark pair in the *s*-channel, mediated by either a W or a left-handed W′ boson, and including interference terms, given as functions of $m_{W'}$ for a relative width of 1% (upper left), 10% (upper right), 20% (lower left), and 30% (lower right). The inner (green) band and the outer (yellow) band indicate the regions containing 68 and 95%, respectively, of the distribution of limits expected under the background-only hypothesis. The solid red curves show the theoretical expectation at LO.

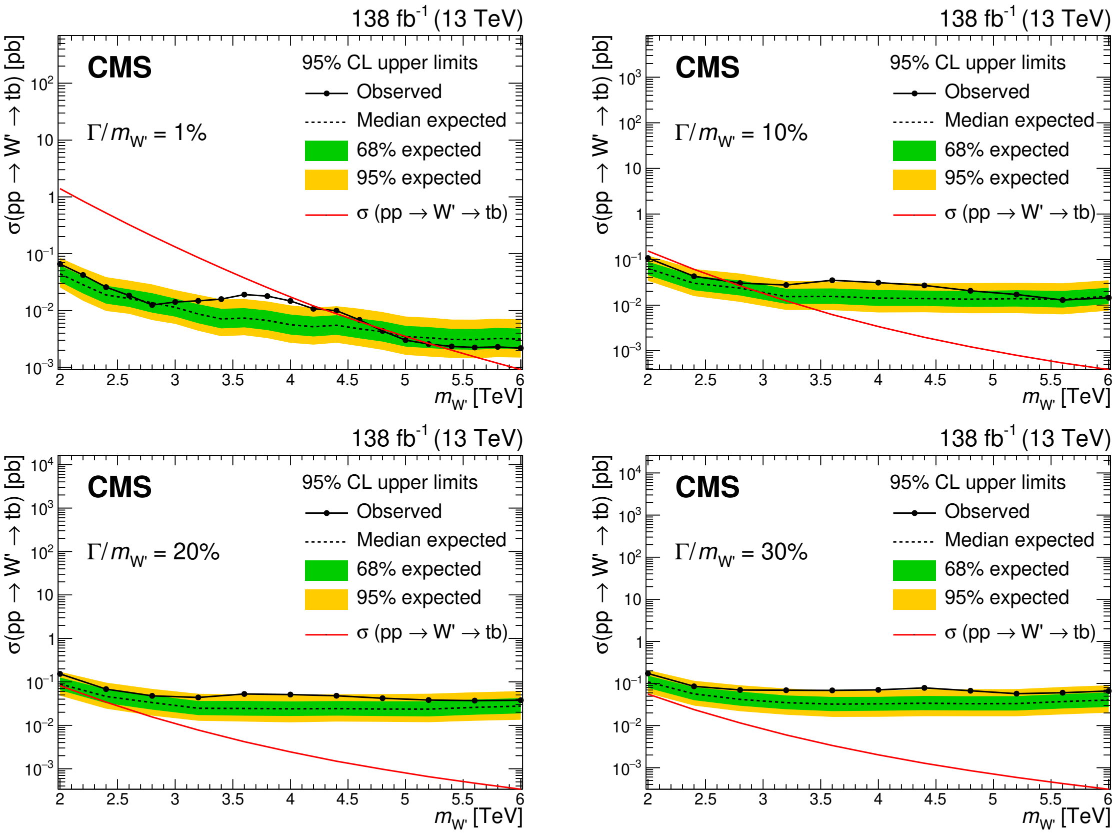

Figure 7: Observed and expected 95% CL upper limits on the product of the production cross section for a right-handed W' boson and the $\mathrm{W}' \to \mathrm{tb}$ branching fraction, as functions of $m_{\mathrm{W}'}$ for a relative width of 1% (upper left), 10% (upper right), 20% (lower left), and 30% (lower right). The inner (green) band and the outer (yellow) band indicate the regions containing 68 and 95%, respectively, of the distribution of limits expected under the background-only hypothesis. The solid red curves show the theoretical expectation at LO.

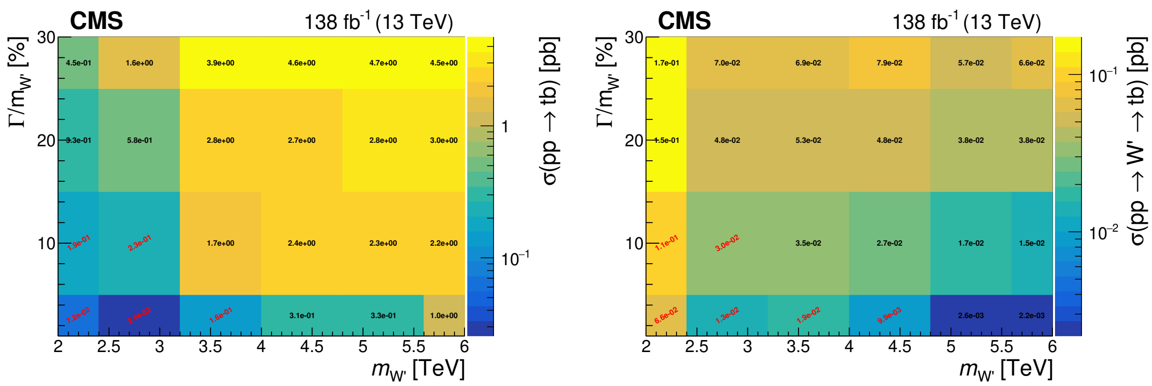

Figure 8: Observed 95% CL upper limit on the production cross section for a left- (on the left) and right-handed (on the right) W' boson in the tb final state, as functions of $m_{\mathrm{W}'}$ and relative width $\Gamma/m_{\mathrm{W}'}$. Numbers in red, written diagonally, represent values of the excluded cross sections that are lower than the theoretical ones for the analyzed model.

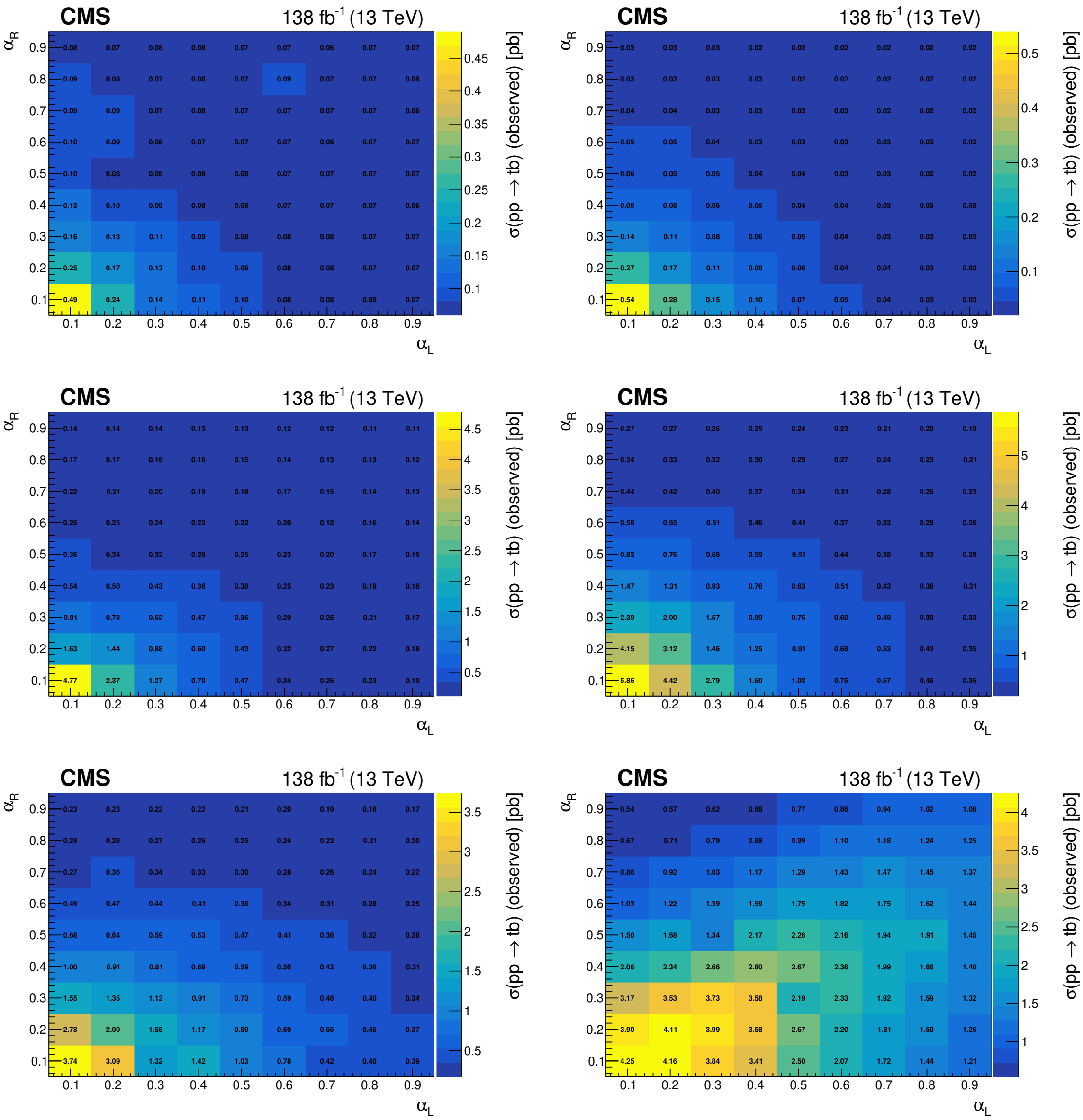

Figure 9: Observed 95% CL upper limit on the production cross section for a generalized left-right coupling of the W′ boson to a t and a b quark for a mass of the W′ boson of 2 TeV (upper left), 2.8 TeV (upper right), 3.6 TeV (middle left), 4.4 TeV (middle right), 5.2 TeV (lower left), and of 6 TeV (lower right).

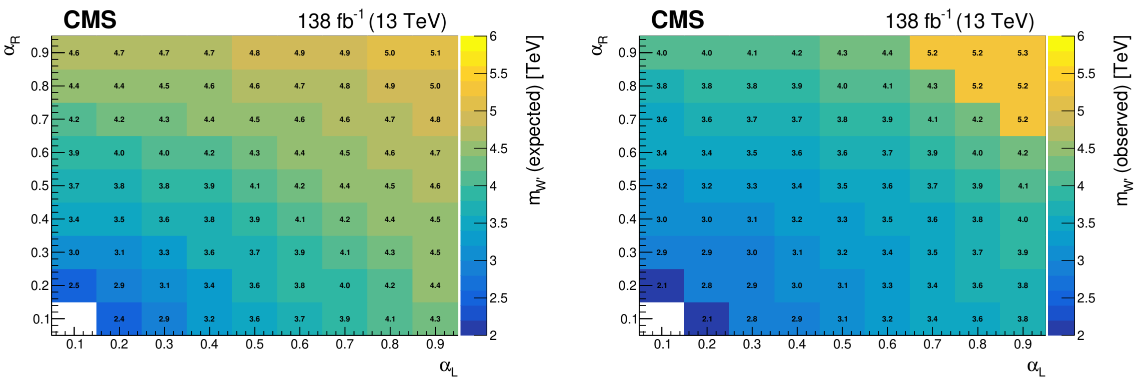

Figure 10: Expected (left) and observed (right) 95% CL lower limit on $m_{\mathrm{W}'}$ for a generalized left-right coupling of the W' boson to a t and a b quark.

11 Summary

A search is presented for W′ bosons decaying to a top and a bottom quark in leptonic final states, making use of 138 fb^{-1} of proton-proton collision data collected with the CMS detector at the LHC. Good agreement between data and the standard model expectation is observed.

Upper limits at 95% confidence level are set on the product of the W′ production cross section and the branching fraction of $W' \to tb$. Multiple hypotheses are considered for the new particle mass, width, and chirality. For a 1% relative width hypothesis, purely right-handed W′ bosons are excluded with masses lower than 4.3 TeV. Production cross sections above 66 to 2 fb are excluded for masses between 2 and 6 TeV. Purely left-handed W′ bosons with a 1% relative decay width are excluded for masses lower than 3.9 TeV.

The largest excess, with a local (global) significance of 2.6 (2.0) standard deviations, is observed for a hypothesized right-handed W′ boson with a mass of 3.8 TeV and a relative width of 1%.

For a 10% relative width hypothesis, purely right-handed W′ bosons are excluded with masses lower than 2.7 TeV. Purely left-handed W′ bosons are excluded with masses lower than 2.5 TeV for a relative width of 10% of the W′ boson mass. For the first time, limits on the production cross section of a W′ boson with relative widths of 20% and 30% are set for purely left- and right-handed couplings. Scenarios with the presence of both left- and right-handed couplings are also tested and limits on their production cross sections are set. For these scenarios, exclusion limits on the W′ boson mass are provided for the considered model.

These results constitute the most stringent constraints to date on a W′ boson decaying to a top and a bottom quark.

Acknowledgments

We congratulate our colleagues in the CERN accelerator departments for the excellent performance of the LHC and thank the technical and administrative staffs at CERN and at other CMS institutes for their contributions to the success of the CMS effort. In addition, we gratefully acknowledge the computing centers and personnel of the Worldwide LHC Computing Grid and other centers for delivering so effectively the computing infrastructure essential to our analyses. Finally, we acknowledge the enduring support for the construction and operation of the LHC, the CMS detector, and the supporting computing infrastructure provided by the following funding agencies: SC (Armenia), BMBWF and FWF (Austria); FNRS and FWO (Belgium); CNPq, CAPES, FAPERJ, FAPERGS, and FAPESP (Brazil); MES and BNSF (Bulgaria); CERN; CAS, MoST, and NSFC (China); MINCIENCIAS (Colombia); MSES and CSF (Croatia); RIF (Cyprus); SENESCYT (Ecuador); MoER, ERC PUT and ERDF (Estonia); Academy of Finland, MEC, and HIP (Finland); CEA and CNRS/IN2P3 (France); SRNSF (Georgia); BMBF, DFG, and HGF (Germany); GSRI (Greece); NKFIH (Hungary); DAE and DST (India); IPM (Iran); SFI (Ireland); INFN (Italy); MSIP and NRF (Republic of Korea); MES (Latvia); LAS (Lithuania); MOE and UM (Malaysia); BUAP, CINVESTAV, CONACYT, LNS, SEP, and UASLP-FAI (Mexico); MOS (Montenegro); MBIE (New Zealand); PAEC (Pakistan); MES and NSC (Poland); FCT (Portugal); MESTD (Serbia); MCIN/AEI and PCTI (Spain); MOSTR (Sri Lanka); Swiss Funding Agencies (Switzerland); MST (Taipei); MHESI and NSTDA (Thailand); TUBITAK and TENMAK (Turkey); NASU (Ukraine); STFC (United Kingdom); DOE and NSF (USA).

Individuals have received support from the Marie-Curie program and the European Research Council and Horizon 2020 Grant, contract Nos. 675440, 724704, 752730, 758316, 765710, 824093, and COST Action CA16108 (European Union); the Leventis Foundation; the Alfred P. Sloan

Foundation; the Alexander von Humboldt Foundation; the Science Committee, project no. 22rl-037 (Armenia); the Belgian Federal Science Policy Office; the Fonds pour la Formation à la Recherche dans l'Industrie et dans l'Agriculture (FRIA-Belgium); the Agentschap voor Innovatie door Wetenschap en Technologie (IWT-Belgium); the F.R.S.-FNRS and FWO (Belgium) under the "Excellence of Science – EOS" – be.h project n. 30820817; the Beijing Municipal Science & Technology Commission, No. Z191100007219010 and Fundamental Research Funds for the Central Universities (China); the Ministry of Education, Youth and Sports (MEYS) of the Czech Republic; the Shota Rustaveli National Science Foundation, grant FR-22-985 (Georgia); the Deutsche Forschungsgemeinschaft (DFG), under Germany's Excellence Strategy – EXC 2121 "Quantum Universe" – 390833306, and under project number 400140256 - GRK2497; the Hellenic Foundation for Research and Innovation (HFRI), Project Number 2288 (Greece); the Hungarian Academy of Sciences, the New National Excellence Program - ÚNKP, the NKFIH research grants K 124845, K 124850, K 128713, K 128786, K 129058, K 131991, K 133046, K 138136, K 143460, K 143477, 2020-2.2.1-ED-2021-00181, and TKP2021-NKTA-64 (Hungary); the Council of Science and Industrial Research, India; ICSC – National Research Center for High Performance Computing, Big Data and Quantum Computing, funded by the EU NexGeneration program (Italy); the Latvian Council of Science; the Ministry of Education and Science, project no. 2022/WK/14, and the National Science Center, contracts Opus 2021/41/B/ST2/01369 and 2021/43/B/ST2/01552 (Poland); the Fundação para a Ciência e a Tecnologia, grant CEECIND/01334/2018 (Portugal); the National Priorities Research Program by Qatar National Research Fund; MCIN/AEI/10.13039/501100011033, ERDF "a way of making Europe", and the Programa Estatal de Fomento de la Investigación Científica y Técnica de Excelencia María de Maeztu, grant MDM-2017-0765 and Programa Severo Ochoa del Principado de Asturias (Spain); the Chulalongkorn Academic into Its 2nd Century Project Advancement Project, and the National Science, Research and Innovation Fund via the Program Management Unit for Human Resources & Institutional Development, Research and Innovation, grant B05F650021 (Thailand); the Kavli Foundation; the Nvidia Corporation; the SuperMicro Corporation; the Welch Foundation, contract C-1845; and the Weston Havens Foundation (USA).

References

[1] R. N. Mohapatra and J. C. Pati, "'Natural' left-right symmetry", *Phys. Rev. D* **11** (1975) 2558, doi:10.1103/PhysRevD.11.2558.

[2] G. Senjanovic and R. N. Mohapatra, "Exact left-right symmetry and spontaneous violation of parity", *Phys. Rev. D* **12** (1975) 1502, doi:10.1103/PhysRevD.12.1502.

[3] P. Minkowski, "$\mu \to e\gamma$ at a rate of one out of 10^9 muon decays?", *Phys. Lett. B* **67** (1977) 421, doi:10.1016/0370-2693(77)90435-X.

[4] R. N. Mohapatra and G. Senjanovic, "Neutrino mass and spontaneous parity nonconservation", *Phys. Rev. Lett.* **44** (1980) 912, doi:10.1103/PhysRevLett.44.912.

[5] J. C. Pati, A. Salam, and J. A. Strathdee, "A preon model with hidden electric and magnetic type charges", *Nucl. Phys. B* **185** (1981) 416, doi:10.1016/0550-3213(81)90327-8.

[6] R. N. Mohapatra, "Unification and Supersymmetry: The Frontiers of Quark-Lepton Physics". Springer, Berlin, 1986. doi:10.1007/978-1-4757-1928-4, ISBN 978-1-4757-1930-7, 978-1-4757-1928-4.

[7] K. S. Babu, X.-G. He, and E. Ma, "New supersymmetric left-right gauge model: Higgs-boson structure and neutral-current analysis", *Phys. Rev. D* **36** (1987) 878, doi:10.1103/PhysRevD.36.878.

[8] F. Pisano and V. Pleitez, "SU(3)⊗U(1) model for electroweak interactions", *Phys. Rev. D* **46** (1992) 410, doi:10.1103/PhysRevD.46.410, arXiv:hep-ph/9206242.

[9] G. Burdman, B. A. Dobrescu, and E. Pontón, "Resonances from two universal extra dimensions", *Phys. Rev. D* **74** (2006) 075008, doi:10.1103/PhysRevD.74.075008, arXiv:hep-ph/0601186.

[10] Z. Chacko, H.-S. Goh, and R. Harnik, "A Twin Higgs model from left-right symmetry", *JHEP* **01** (2006) 108, doi:10.1088/1126-6708/2006/01/108, arXiv:hep-ph/0512088.

[11] H.-S. Goh and C. A. Krenke, "Little Twin Higgs model", *Phys. Rev. D* **76** (2007) 115018, doi:10.1103/PhysRevD.76.115018, arXiv:0707.3650.

[12] A. Belyaev et al., "Technicolor Walks at the LHC", *Phys. Rev. D* **79** (2009) 035006, doi:10.1103/PhysRevD.79.035006, arXiv:0809.0793.

[13] J. M. Cabarcas, D. Gomez Dumm, and R. Martinez, "Flavor changing neutral currents in 331 models", *J. Phys. G* **37** (2010) 045001, doi:10.1088/0954-3899/37/4/045001, arXiv:0910.5700.

[14] A. J. Buras, F. De Fazio, J. Girrbach, and M. V. Carlucci, "The anatomy of quark flavour observables in 331 models in the flavour precision era", *JHEP* **02** (2013) 023, doi:10.1007/JHEP02(2013)023, arXiv:1211.1237.

[15] A. Ahmed, "Heavy Higgs of the Twin Higgs models", *JHEP* **02** (2018) 048, doi:10.1007/JHEP02(2018)048, arXiv:1711.03107.

[16] BABAR Collaboration, "Evidence for an excess of $\bar{B} \to D^{(*)}\tau^-\bar{\nu}_\tau$ decays", *Phys. Rev. Lett.* **109** (2012) 101802, doi:10.1103/PhysRevLett.109.101802, arXiv:1205.5442.

[17] Belle Collaboration, "Measurement of the τ lepton polarization and $R(D^*)$ in the decay $\bar{B} \to D^*\tau^-\bar{\nu}_\tau$", *Phys. Rev. Lett.* **118** (2017) 211801, doi:10.1103/PhysRevLett.118.211801, arXiv:1612.00529.

[18] M. Abdullah et al., "Probing a simplified W′ model of $R(D^*)$ anomalies using b tags, τ leptons, and missing energy", *Phys. Rev. D* **98** (2018) 055016, doi:10.1103/PhysRevD.98.055016, arXiv:1805.01869.

[19] D. J. Muller and S. Nandi, "Top flavor: A separate SU(2) for the third family", *Phys. Lett. B* **383** (1996) 345, doi:10.1016/0370-2693(96)00745-9, arXiv:hep-ph/9602390.

[20] R. Calabrese et al., "Top-flavor scheme in the context of W′ searches at LHC", *Phys. Rev. D* **104** (2021) 055006, doi:10.1103/PhysRevD.104.055006, arXiv:2104.06720.

[21] CMS Collaboration, "Search for heavy resonances decaying to a top quark and a bottom quark in the lepton+jets final state in proton-proton collisions at 13 TeV", *Phys. Lett. B* **777** (2018) 39, doi:10.1016/j.physletb.2017.12.006, arXiv:1708.08539.

[22] ATLAS Collaboration, "Search for high-mass resonances decaying to $\tau\nu$ in pp collisions at $\sqrt{s} = 13$ TeV with the ATLAS detector", *Phys. Rev. Lett.* **120** (2018) 161802, doi:10.1103/PhysRevLett.120.161802, arXiv:1801.06992.

[23] ATLAS Collaboration, "Search for vector-boson resonances decaying to a top quark and bottom quark in the lepton plus jets final state in pp collisions at $\sqrt{s} = 13$ TeV with the ATLAS detector", *Phys. Lett. B* **788** (2019) 347, doi:10.1016/j.physletb.2018.11.032, arXiv:1807.10473.

[24] CMS Collaboration, "Search for a W′ boson decaying to a τ lepton and a neutrino in proton-proton collisions at $\sqrt{s} = 13$ TeV", *Phys. Lett. B* **792** (2019) 107, doi:10.1016/j.physletb.2019.01.069, arXiv:1807.11421.

[25] CMS Collaboration, "Search for W′ bosons decaying to a top and a bottom quark at $\sqrt{s} = 13$ TeV in the hadronic final state", *Phys. Lett. B* **820** (2021) 136535, doi:10.1016/j.physletb.2021.136535, arXiv:2104.04831.

[26] N. Vignaroli, "New W′ signals at the LHC", *Phys. Rev. D* **89** (2014) 095027, doi:10.1103/PhysRevD.89.095027, arXiv:1404.5558.

[27] D. Barducci and C. Delaunay, "Bounding wide composite vector resonances at the LHC", *JHEP* **02** (2016) 055, doi:10.1007/JHEP02(2016)055, arXiv:1511.01101.

[28] "HEPData record for this analysis", 2023. doi:10.17182/hepdata.144179.

[29] CMS Collaboration, "The CMS experiment at the CERN LHC", *JINST* **3** (2008) S08004, doi:10.1088/1748-0221/3/08/S08004.

[30] CMS Collaboration, "The CMS trigger system", *JINST* **12** (2017) P01020, doi:10.1088/1748-0221/12/01/P01020, arXiv:1609.02366.

[31] J. Alwall et al., "The automated computation of tree-level and next-to-leading order differential cross sections, and their matching to parton shower simulations", *JHEP* **07** (2014) 079, doi:10.1007/JHEP07(2014)079, arXiv:1405.0301.

[32] P. Nason, "A new method for combining NLO QCD with shower Monte Carlo algorithms", *JHEP* **11** (2004) 040, doi:10.1088/1126-6708/2004/11/040, arXiv:hep-ph/0409146.

[33] S. Frixione, P. Nason, and C. Oleari, "Matching NLO QCD computations with parton shower simulations: the POWHEG method", *JHEP* **11** (2007) 070, doi:10.1088/1126-6708/2007/11/070, arXiv:0709.2092.

[34] S. Alioli, P. Nason, C. Oleari, and E. Re, "A general framework for implementing NLO calculations in shower Monte Carlo programs: the POWHEG BOX", *JHEP* **06** (2010) 043, doi:10.1007/JHEP06(2010)043, arXiv:1002.2581.

[35] S. Frixione, P. Nason, and G. Ridolfi, "A positive-weight next-to-leading-order Monte Carlo for heavy flavour hadroproduction", *JHEP* **09** (2007) 126, doi:10.1088/1126-6708/2007/09/126, arXiv:0707.3088.

[36] R. Frederix, E. Re, and P. Torrielli, "Single-top t-channel hadroproduction in the four-flavour scheme with POWHEG and aMC@NLO", *JHEP* **09** (2012) 130, doi:10.1007/JHEP09(2012)130, arXiv:1207.5391.

[37] CMS Collaboration, "Event generator tunes obtained from underlying event and multiparton scattering measurements", *Eur. Phys. J. C* **76** (2016) 155, doi:10.1140/epjc/s10052-016-3988-x, arXiv:1512.00815.

[38] CMS Collaboration, "Extraction and validation of a new set of CMS PYTHIA8 tunes from underlying-event measurements", *Eur. Phys. J. C* **80** (2020) 4, doi:10.1140/epjc/s10052-019-7499-4, arXiv:1903.12179.

[39] CMS Collaboration, "Investigations of the impact of the parton shower tuning in PYTHIA 8 in the modelling of $\mathrm{t\bar{t}}$ at $\sqrt{s} = 8$ and 13 TeV", CMS Physics Analysis Summary CMS-PAS-TOP-16-021, 2016.

[40] M. Czakon and A. Mitov, "Top++: a program for the calculation of the top-pair cross-section at hadron colliders", *Comput. Phys. Commun.* **185** (2014) 2930, doi:10.1016/j.cpc.2014.06.021, arXiv:1112.5675.

[41] M. Aliev et al., "HATHOR — HAdronic Top and Heavy quarks crOss section calculatoR", *Comput. Phys. Commun.* **182** (2011) 1034, doi:10.1016/j.cpc.2010.12.040, arXiv:1007.1327.

[42] J. M. Lindert et al., "Precise predictions for V+jets dark matter backgrounds", *Eur. Phys. J. C* **77** (2017) 829, doi:10.1140/epjc/s10052-017-5389-1, arXiv:1705.04664.

[43] CMS Collaboration, "Search for a W′ boson decaying to a bottom quark and a top quark in pp collisions at $\sqrt{s} = 7$ TeV", *Phys. Lett. B* **718** (2013) 1229, doi:10.1016/j.physletb.2012.12.008, arXiv:1208.0956.

[44] NNPDF Collaboration, "Parton distributions for the LHC Run II", *JHEP* **04** (2015) 040, doi:10.1007/JHEP04(2015)040, arXiv:1410.8849.

[45] NNPDF Collaboration, "Parton distributions from high-precision collider data", *Eur. Phys. J. C* **77** (2017) 663, doi:10.1140/epjc/s10052-017-5199-5, arXiv:1706.00428.

[46] GEANT4 Collaboration, "GEANT4—a simulation toolkit", *Nucl. Instrum. Meth. A* **506** (2003) 250, doi:10.1016/S0168-9002(03)01368-8.

[47] CMS Collaboration, "Particle-flow reconstruction and global event description with the CMS detector", *JINST* **12** (2017) P10003, doi:10.1088/1748-0221/12/10/P10003, arXiv:1706.04965.

[48] CMS Collaboration, "Technical proposal for the Phase-II upgrade of the Compact Muon Solenoid", CMS Technical Proposal CERN-LHCC-2015-010, CMS-TDR-15-02, 2015.

[49] M. Cacciari, G. P. Salam, and G. Soyez, "The anti-k_{T} jet clustering algorithm", *JHEP* **04** (2008) 063, doi:10.1088/1126-6708/2008/04/063, arXiv:0802.1189.

[50] M. Cacciari, G. P. Salam, and G. Soyez, "FastJet user manual", *Eur. Phys. J. C* **72** (2012) 1896, doi:10.1140/epjc/s10052-012-1896-2, arXiv:1111.6097.

[51] K. Rehermann and B. Tweedie, "Efficient identification of boosted semileptonic top quarks at the LHC", *JHEP* **03** (2011) 059, doi:10.1007/JHEP03(2011)059, arXiv:1007.2221.

[52] J. M. Butterworth, A. R. Davison, M. Rubin, and G. P. Salam, "Jet substructure as a new Higgs search channel at the LHC", *Phys. Rev. Lett.* **100** (2008) 242001, doi:10.1103/PhysRevLett.100.242001, arXiv:0802.2470.

[53] M. Dasgupta, A. Fregoso, S. Marzani, and G. P. Salam, "Towards an understanding of jet substructure", *JHEP* **09** (2013) 029, doi:10.1007/JHEP09(2013)029, arXiv:1307.0007.

[54] A. J. Larkoski, S. Marzani, G. Soyez, and J. Thaler, "Soft drop", *JHEP* **05** (2014) 146, doi:10.1007/JHEP05(2014)146, arXiv:1402.2657.

[55] M. Cacciari and G. P. Salam, "Pileup subtraction using jet areas", *Phys. Lett. B* **659** (2008) 119, doi:10.1016/j.physletb.2007.09.077, arXiv:0707.1378.

[56] D. Bertolini, P. Harris, M. Low, and N. Tran, "Pileup per particle identification", *JHEP* **10** (2014) 059, doi:10.1007/JHEP10(2014)059, arXiv:1407.6013.

[57] CMS Collaboration, "Jet energy scale and resolution in the CMS experiment in pp collisions at 8 TeV", *JINST* **12** (2017) P02014, doi:10.1088/1748-0221/12/02/P02014, arXiv:1607.03663.

[58] CMS Collaboration, "Jet algorithms performance in 13 TeV data", technical report, CERN, Geneva, 2017.

[59] CMS Collaboration, "Identification of heavy-flavour jets with the CMS detector in pp collisions at 13 TeV", *JINST* **13** (2018) P05011, doi:10.1088/1748-0221/13/05/P05011, arXiv:1712.07158.

[60] CMS Collaboration, "Performance of the DeepJet b tagging algorithm using 41.9/fb of data from proton-proton collisions at 13 TeV with Phase 1 CMS detector", CMS Detector Performance Note CMS-DP-2018-058, 2018.

[61] E. Bols et al., "Jet flavour classification using DeepJet", *JINST* **15** (2020) P12012, doi:10.1088/1748-0221/15/12/P12012, arXiv:2008.10519.

[62] CMS Collaboration, "Measurement of the single top quark and antiquark production cross sections in the t channel and their ratio in proton-proton collisions at $\sqrt{s} = 13$ TeV", *Phys. Lett. B* **800** (2019) 135042, doi:10.1016/j.physletb.2019.135042, arXiv:1812.10514.

[63] Particle Data Group Collaboration, "Review of particle physics", *Prog. Theor. Exp. Phys.* **2022** (2022) 083C01, doi:10.1093/ptep/ptac097.

[64] CMS Collaboration, "Precision luminosity measurement in proton-proton collisions at $\sqrt{s} = 13$ TeV in 2015 and 2016 at CMS", *Eur. Phys. J. C* **81** (2021) 800, doi:10.1140/epjc/s10052-021-09538-2, arXiv:2104.01927.

[65] CMS Collaboration, "CMS luminosity measurement for the 2017 data-taking period at $\sqrt{s} = 13$ TeV", CMS Physics Analysis Summary CMS-PAS-LUM-17-004, 2018.

[66] CMS Collaboration, "CMS luminosity measurement for the 2018 data-taking period at $\sqrt{s} = 13\,\text{TeV}$", CMS Physics Analysis Summary CMS-PAS-LUM-18-002, 2019.

[67] J. Butterworth et al., "PDF4LHC recommendations for LHC Run II", *J. Phys. G* **43** (2016) 023001, doi:10.1088/0954-3899/43/2/023001, arXiv:1510.03865.

[68] CMS Collaboration, "Measurement of the inelastic proton-proton cross section at $\sqrt{s} = 13\,\text{TeV}$", *JHEP* **07** (2018) 161, doi:10.1007/JHEP07(2018)161, arXiv:1802.02613.

[69] R. Barlow and C. Beeston, "Fitting using finite Monte Carlo samples", *Comput. Phys. Commun.* **77** (1993) 219, doi:10.1016/0010-4655(93)90005-W.

[70] J. S. Conway, "Nuisance parameters in likelihoods for multisource spectra", in *Proceedings of PHYSTAT 2011 Workshop on Statistical Issues Related to Discovery Claims in Search Experiments and Unfolding*, H. Prosper and L. Lyons, eds., number CERN-2011-006, p. 115. CERN, 2011.

[71] E. Gross and O. Vitells, "Trial factors for the look elsewhere effect in high energy physics", *Eur. Phys. J. C* **70** (2010) 525, doi:10.1140/epjc/s10052-010-1470-8, arXiv:1005.1891.

[72] T. Junk, "Confidence level computation for combining searches with small statistics", *Nucl. Instrum. Meth. A* **434** (1999) 435, doi:10.1016/S0168-9002(99)00498-2, arXiv:hep-ex/9902006.

[73] A. L. Read, "Presentation of search results: the CL_s technique", *J. Phys. G* **28** (2002) 2693, doi:10.1088/0954-3899/28/10/313.

[74] G. Cowan, K. Cranmer, E. Gross, and O. Vitells, "Asymptotic formulae for likelihood-based tests of new physics", *Eur. Phys. J. C* **71** (2011) 1554, doi:10.1140/epjc/s10052-011-1554-0, arXiv:1007.1727. [Erratum: doi:10.1140/epjc/s10052-013-2501-z].

[75] E. Boos, V. Bunichev, L. Dudko, and M. Perfilov, "Interference between W' and W in single-top quark production processes", *Phys. Lett. B* **655** (2007) 245, doi:10.1016/j.physletb.2007.03.064, arXiv:hep-ph/0610080.

A Alternative cross sections

Upper limits are also provided in the case that the couplings, and thus the partial widths, are varied together with the total width. In this interpretation the branching fraction of the W′ → tb decays is the same for each value of the width of the W′ boson, where no additional decays are hypothesized, but the coupling strength is increased by a factor $(\Gamma/m_{W'})^2$. Figure A.1 shows the limits for an RH W′ boson with these alternative theoretical cross sections.

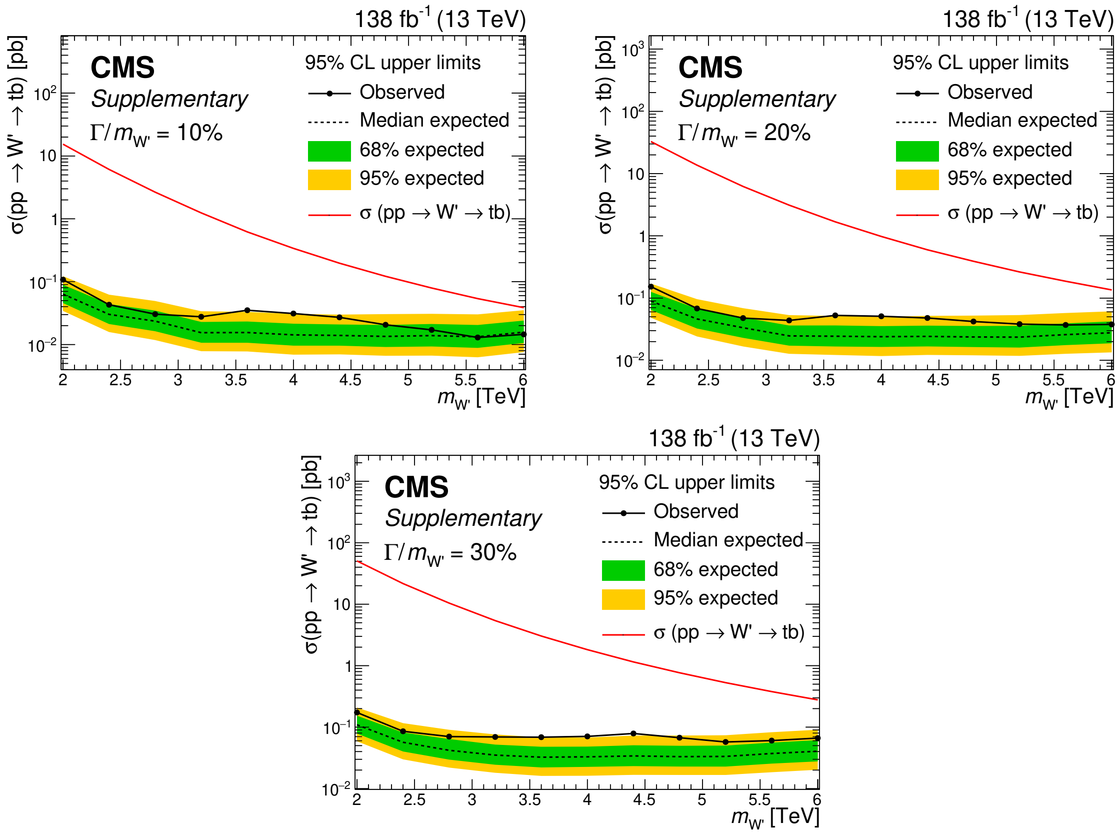

Figure A.1: Observed and expected 95% CL upper limits on the product of the production cross section for a right-handed W′ boson and the W′ → tb branching fraction, as functions of the $m_{W'}$ for a relative width of 10% (upper left), 20% (upper right), and 30% (lower).. The inner (green) band and the outer (yellow) band indicate the regions containing 68 and 95%, respectively, of the distribution of limits expected under the background-only hypothesis. The solid curves show the theoretical expectation at LO in the case that the couplings, and thus the partial widths, are varied together with the total width. In this interpretation the branching fraction of the W′ → tb decays is the same for each value of the width of the W′ boson.

B The CMS Collaboration

Yerevan Physics Institute, Yerevan, Armenia
A. Hayrapetyan, A. Tumasyan[1]

Institut für Hochenergiephysik, Vienna, Austria
W. Adam, J.W. Andrejkovic, T. Bergauer, S. Chatterjee, K. Damanakis, M. Dragicevic, A. Escalante Del Valle, P.S. Hussain, M. Jeitler[2], N. Krammer, D. Liko, I. Mikulec, J. Schieck[2], R. Schöfbeck, D. Schwarz, M. Sonawane, S. Templ, W. Waltenberger, C.-E. Wulz[2]

Universiteit Antwerpen, Antwerpen, Belgium
M.R. Darwish[3], T. Janssen, P. Van Mechelen

Vrije Universiteit Brussel, Brussel, Belgium
E.S. Bols, J. D'Hondt, S. Dansana, A. De Moor, M. Delcourt, H. El Faham, S. Lowette, I. Makarenko, D. Müller, A.R. Sahasransu, S. Tavernier, M. Tytgat[4], S. Van Putte, D. Vannerom

Université Libre de Bruxelles, Bruxelles, Belgium
B. Clerbaux, G. De Lentdecker, L. Favart, D. Hohov, J. Jaramillo, A. Khalilzadeh, K. Lee, M. Mahdavikhorrami, A. Malara, S. Paredes, L. Pétré, N. Postiau, L. Thomas, M. Vanden Bemden, C. Vander Velde, P. Vanlaer

Ghent University, Ghent, Belgium
M. De Coen, D. Dobur, Y. Hong, J. Knolle, L. Lambrecht, G. Mestdach, C. Rendón, A. Samalan, K. Skovpen, N. Van Den Bossche, L. Wezenbeek

Université Catholique de Louvain, Louvain-la-Neuve, Belgium
A. Benecke, G. Bruno, C. Caputo, C. Delaere, I.S. Donertas, A. Giammanco, K. Jaffel, Sa. Jain, V. Lemaitre, J. Lidrych, P. Mastrapasqua, K. Mondal, T.T. Tran, S. Wertz

Centro Brasileiro de Pesquisas Fisicas, Rio de Janeiro, Brazil
G.A. Alves, E. Coelho, C. Hensel, T. Menezes De Oliveira, A. Moraes, P. Rebello Teles, M. Soeiro

Universidade do Estado do Rio de Janeiro, Rio de Janeiro, Brazil
W.L. Aldá Júnior, M. Alves Gallo Pereira, M. Barroso Ferreira Filho, H. Brandao Malbouisson, W. Carvalho, J. Chinellato[5], E.M. Da Costa, G.G. Da Silveira[6], D. De Jesus Damiao, S. Fonseca De Souza, J. Martins[7], C. Mora Herrera, K. Mota Amarilo, L. Mundim, H. Nogima, A. Santoro, S.M. Silva Do Amaral, A. Sznajder, M. Thiel, A. Vilela Pereira

Universidade Estadual Paulista, Universidade Federal do ABC, São Paulo, Brazil
C.A. Bernardes[6], L. Calligaris, T.R. Fernandez Perez Tomei, E.M. Gregores, P.G. Mercadante, S.F. Novaes, B. Orzari, Sandra S. Padula

Institute for Nuclear Research and Nuclear Energy, Bulgarian Academy of Sciences, Sofia, Bulgaria
A. Aleksandrov, G. Antchev, R. Hadjiiska, P. Iaydjiev, M. Misheva, M. Shopova, G. Sultanov

University of Sofia, Sofia, Bulgaria
A. Dimitrov, T. Ivanov, L. Litov, B. Pavlov, P. Petkov, A. Petrov, E. Shumka

Instituto De Alta Investigación, Universidad de Tarapacá, Casilla 7 D, Arica, Chile
S. Keshri, S. Thakur

Beihang University, Beijing, China
T. Cheng, Q. Guo, T. Javaid, M. Mittal, L. Yuan

Department of Physics, Tsinghua University, Beijing, China
G. Bauer[8], Z. Hu, K. Yi[8,9]

Institute of High Energy Physics, Beijing, China
G.M. Chen[10], H.S. Chen[10], M. Chen[10], F. Iemmi, C.H. Jiang, A. Kapoor, H. Liao, Z.-A. Liu[11], F. Monti, R. Sharma, J.N. Song[11], J. Tao, C. Wang[10], J. Wang, Z. Wang[10], H. Zhang

State Key Laboratory of Nuclear Physics and Technology, Peking University, Beijing, China
A. Agapitos, Y. Ban, A. Levin, C. Li, Q. Li, X. Lyu, Y. Mao, S.J. Qian, X. Sun, D. Wang, H. Yang, C. Zhou

Sun Yat-Sen University, Guangzhou, China
Z. You

University of Science and Technology of China, Hefei, China
N. Lu

Institute of Modern Physics and Key Laboratory of Nuclear Physics and Ion-beam Application (MOE) - Fudan University, Shanghai, China
D. Leggat, H. Okawa, Y. Zhang

Zhejiang University, Hangzhou, Zhejiang, China
Z. Lin, C. Lu, M. Xiao

Universidad de Los Andes, Bogota, Colombia
C. Avila, D.A. Barbosa Trujillo, A. Cabrera, C. Florez, J. Fraga, J.A. Reyes Vega

Universidad de Antioquia, Medellin, Colombia
J. Mejia Guisao, F. Ramirez, M. Rodriguez, J.D. Ruiz Alvarez

University of Split, Faculty of Electrical Engineering, Mechanical Engineering and Naval Architecture, Split, Croatia
D. Giljanovic, N. Godinovic, D. Lelas, A. Sculac

University of Split, Faculty of Science, Split, Croatia
M. Kovac, T. Sculac

Institute Rudjer Boskovic, Zagreb, Croatia
P. Bargassa, V. Brigljevic, B.K. Chitroda, D. Ferencek, S. Mishra, A. Starodumov[12], T. Susa

University of Cyprus, Nicosia, Cyprus
A. Attikis, K. Christoforou, S. Konstantinou, J. Mousa, C. Nicolaou, F. Ptochos, P.A. Razis, H. Rykaczewski, H. Saka, A. Stepennov

Charles University, Prague, Czech Republic
M. Finger, M. Finger Jr., A. Kveton

Escuela Politecnica Nacional, Quito, Ecuador
E. Ayala

Universidad San Francisco de Quito, Quito, Ecuador
E. Carrera Jarrin

Academy of Scientific Research and Technology of the Arab Republic of Egypt, Egyptian Network of High Energy Physics, Cairo, Egypt
Y. Assran[13,14], S. Elgammal[14]

Center for High Energy Physics (CHEP-FU), Fayoum University, El-Fayoum, Egypt
M. Abdullah Al-Mashad, M.A. Mahmoud

National Institute of Chemical Physics and Biophysics, Tallinn, Estonia
R.K. Dewanjee[15], K. Ehataht, M. Kadastik, T. Lange, S. Nandan, C. Nielsen, J. Pata, M. Raidal, L. Tani, C. Veelken

Department of Physics, University of Helsinki, Helsinki, Finland
H. Kirschenmann, K. Osterberg, M. Voutilainen

Helsinki Institute of Physics, Helsinki, Finland
S. Bharthuar, E. Brücken, F. Garcia, J. Havukainen, K.T.S. Kallonen, M.S. Kim, R. Kinnunen, T. Lampén, K. Lassila-Perini, S. Lehti, T. Lindén, M. Lotti, L. Martikainen, M. Myllymäki, M.m. Rantanen, H. Siikonen, E. Tuominen, J. Tuominiemi

Lappeenranta-Lahti University of Technology, Lappeenranta, Finland
P. Luukka, H. Petrow, T. Tuuva[†]

IRFU, CEA, Université Paris-Saclay, Gif-sur-Yvette, France
M. Besancon, F. Couderc, M. Dejardin, D. Denegri, J.L. Faure, F. Ferri, S. Ganjour, P. Gras, G. Hamel de Monchenault, V. Lohezic, J. Malcles, J. Rander, A. Rosowsky, M.Ö. Sahin, A. Savoy-Navarro[16], P. Simkina, M. Titov

Laboratoire Leprince-Ringuet, CNRS/IN2P3, Ecole Polytechnique, Institut Polytechnique de Paris, Palaiseau, France
C. Baldenegro Barrera, F. Beaudette, A. Buchot Perraguin, P. Busson, A. Cappati, C. Charlot, F. Damas, O. Davignon, A. De Wit, G. Falmagne, B.A. Fontana Santos Alves, S. Ghosh, A. Gilbert, R. Granier de Cassagnac, A. Hakimi, B. Harikrishnan, L. Kalipoliti, G. Liu, J. Motta, M. Nguyen, C. Ochando, L. Portales, R. Salerno, U. Sarkar, J.B. Sauvan, Y. Sirois, A. Tarabini, E. Vernazza, A. Zabi, A. Zghiche

Université de Strasbourg, CNRS, IPHC UMR 7178, Strasbourg, France
J.-L. Agram[17], J. Andrea, D. Apparu, D. Bloch, J.-M. Brom, E.C. Chabert, C. Collard, S. Falke, U. Goerlach, C. Grimault, R. Haeberle, A.-C. Le Bihan, M.A. Sessini, P. Van Hove

Institut de Physique des 2 Infinis de Lyon (IP2I), Villeurbanne, France
S. Beauceron, B. Blancon, G. Boudoul, N. Chanon, J. Choi, D. Contardo, P. Depasse, C. Dozen[18], H. El Mamouni, J. Fay, S. Gascon, M. Gouzevitch, C. Greenberg, G. Grenier, B. Ille, I.B. Laktineh, M. Lethuillier, L. Mirabito, S. Perries, M. Vander Donckt, P. Verdier, J. Xiao

Georgian Technical University, Tbilisi, Georgia
I. Lomidze, T. Toriashvili[19], Z. Tsamalaidze[12]

RWTH Aachen University, I. Physikalisches Institut, Aachen, Germany

V. Botta, L. Feld, K. Klein, M. Lipinski, D. Meuser, A. Pauls, N. Röwert, M. Teroerde

RWTH Aachen University, III. Physikalisches Institut A, Aachen, Germany
S. Diekmann, A. Dodonova, N. Eich, D. Eliseev, F. Engelke, M. Erdmann, P. Fackeldey, B. Fischer, T. Hebbeker, K. Hoepfner, F. Ivone, A. Jung, M.y. Lee, L. Mastrolorenzo, M. Merschmeyer, A. Meyer, S. Mukherjee, D. Noll, A. Novak, F. Nowotny, A. Pozdnyakov, Y. Rath, W. Redjeb, F. Rehm, H. Reithler, V. Sarkisovi, A. Schmidt, S.C. Schuler, A. Sharma, A. Stein, F. Torres Da Silva De Araujo[20], L. Vigilante, S. Wiedenbeck, S. Zaleski

RWTH Aachen University, III. Physikalisches Institut B, Aachen, Germany
C. Dziwok, G. Flügge, W. Haj Ahmad[21], T. Kress, A. Nowack, O. Pooth, A. Stahl, T. Ziemons, A. Zotz

Deutsches Elektronen-Synchrotron, Hamburg, Germany
H. Aarup Petersen, M. Aldaya Martin, J. Alimena, S. Amoroso, Y. An, S. Baxter, M. Bayatmakou, H. Becerril Gonzalez, O. Behnke, A. Belvedere, S. Bhattacharya, F. Blekman[22], K. Borras[23], D. Brunner, A. Campbell, A. Cardini, C. Cheng, F. Colombina, S. Consuegra Rodríguez, G. Correia Silva, M. De Silva, G. Eckerlin, D. Eckstein, L.I. Estevez Banos, O. Filatov, E. Gallo[22], A. Geiser, A. Giraldi, G. Greau, V. Guglielmi, M. Guthoff, A. Hinzmann, A. Jafari[24], L. Jeppe, N.Z. Jomhari, B. Kaech, M. Kasemann, H. Kaveh, C. Kleinwort, R. Kogler, M. Komm, D. Krücker, W. Lange, D. Leyva Pernia, K. Lipka[25], W. Lohmann[26], R. Mankel, I.-A. Melzer-Pellmann, M. Mendizabal Morentin, J. Metwally, A.B. Meyer, G. Milella, A. Mussgiller, A. Nürnberg, Y. Otarid, D. Pérez Adán, E. Ranken, A. Raspereza, B. Ribeiro Lopes, J. Rübenach, A. Saggio, M. Scham[27,23], V. Scheurer, S. Schnake[23], P. Schütze, C. Schwanenberger[22], M. Shchedrolosiev, R.E. Sosa Ricardo, L.P. Sreelatha Pramod, D. Stafford, F. Vazzoler, A. Ventura Barroso, R. Walsh, Q. Wang, Y. Wen, K. Wichmann, L. Wiens[23], C. Wissing, S. Wuchterl, Y. Yang, A. Zimermmane Castro Santos

University of Hamburg, Hamburg, Germany
A. Albrecht, S. Albrecht, M. Antonello, S. Bein, L. Benato, M. Bonanomi, P. Connor, M. Eich, K. El Morabit, Y. Fischer, A. Fröhlich, C. Garbers, E. Garutti, A. Grohsjean, M. Hajheidari, J. Haller, H.R. Jabusch, G. Kasieczka, P. Keicher, R. Klanner, W. Korcari, T. Kramer, V. Kutzner, F. Labe, J. Lange, A. Lobanov, C. Matthies, A. Mehta, L. Moureaux, M. Mrowietz, A. Nigamova, Y. Nissan, A. Paasch, K.J. Pena Rodriguez, T. Quadfasel, B. Raciti, M. Rieger, D. Savoiu, J. Schindler, P. Schleper, M. Schröder, J. Schwandt, M. Sommerhalder, H. Stadie, G. Steinbrück, A. Tews, M. Wolf

Karlsruher Institut fuer Technologie, Karlsruhe, Germany
S. Brommer, M. Burkart, E. Butz, T. Chwalek, A. Dierlamm, A. Droll, N. Faltermann, M. Giffels, A. Gottmann, F. Hartmann[28], M. Horzela, U. Husemann, M. Klute, R. Koppenhöfer, M. Link, A. Lintuluoto, S. Maier, S. Mitra, M. Mormile, Th. Müller, M. Neukum, M. Oh, G. Quast, K. Rabbertz, I. Shvetsov, H.J. Simonis, N. Trevisani, R. Ulrich, J. van der Linden, R.F. Von Cube, M. Wassmer, S. Wieland, F. Wittig, R. Wolf, S. Wunsch, X. Zuo

Institute of Nuclear and Particle Physics (INPP), NCSR Demokritos, Aghia Paraskevi, Greece

G. Anagnostou, P. Assiouras, G. Daskalakis, A. Kyriakis, A. Papadopoulos[28], A. Stakia

National and Kapodistrian University of Athens, Athens, Greece
D. Karasavvas, P. Kontaxakis, G. Melachroinos, A. Panagiotou, I. Papavergou, I. Paraskevas, N. Saoulidou, K. Theofilatos, E. Tziaferi, K. Vellidis, I. Zisopoulos

National Technical University of Athens, Athens, Greece
G. Bakas, T. Chatzistavrou, G. Karapostoli, K. Kousouris, I. Papakrivopoulos, E. Siamarkou, G. Tsipolitis, A. Zacharopoulou

University of Ioánnina, Ioánnina, Greece
K. Adamidis, I. Bestintzanos, I. Evangelou, C. Foudas, P. Gianneios, C. Kamtsikis, P. Katsoulis, P. Kokkas, P.G. Kosmoglou Kioseoglou, N. Manthos, I. Papadopoulos, J. Strologas

HUN-REN Wigner Research Centre for Physics, Budapest, Hungary
M. Bartók[29], C. Hajdu, D. Horvath[30,31], F. Sikler, V. Veszpremi

MTA-ELTE Lendület CMS Particle and Nuclear Physics Group, Eötvös Loránd University, Budapest, Hungary
M. Csanád, K. Farkas, M.M.A. Gadallah[32], Á. Kadlecsik, P. Major, K. Mandal, G. Pásztor, A.J. Rádl[33], G.I. Veres

Faculty of Informatics, University of Debrecen, Debrecen, Hungary
P. Raics, B. Ujvari[34], G. Zilizi

Institute of Nuclear Research ATOMKI, Debrecen, Hungary
G. Bencze, S. Czellar, J. Karancsi[29], J. Molnar, Z. Szillasi

Karoly Robert Campus, MATE Institute of Technology, Gyongyos, Hungary
T. Csorgo[33], F. Nemes[33], T. Novak

Panjab University, Chandigarh, India
J. Babbar, S. Bansal, S.B. Beri, V. Bhatnagar, G. Chaudhary, S. Chauhan, N. Dhingra[35], R. Gupta, A. Kaur, A. Kaur, H. Kaur, M. Kaur, S. Kumar, P. Kumari, M. Meena, K. Sandeep, T. Sheokand, J.B. Singh[36], A. Singla

University of Delhi, Delhi, India
A. Ahmed, A. Bhardwaj, A. Chhetri, B.C. Choudhary, A. Kumar, M. Naimuddin, K. Ranjan, S. Saumya

Saha Institute of Nuclear Physics, HBNI, Kolkata, India
S. Baradia, S. Barman[37], S. Bhattacharya, D. Bhowmik, S. Dutta, S. Dutta, B. Gomber[38], P. Palit, G. Saha, B. Sahu[38], S. Sarkar

Indian Institute of Technology Madras, Madras, India
M.M. Ameen, P.K. Behera, S.C. Behera, S. Chatterjee, P. Jana, P. Kalbhor, J.R. Komaragiri[39], D. Kumar[39], L. Panwar[39], R. Pradhan, P.R. Pujahari, N.R. Saha, A. Sharma, A.K. Sikdar, S. Verma

Tata Institute of Fundamental Research-A, Mumbai, India
T. Aziz, I. Das, S. Dugad, M. Kumar, G.B. Mohanty, P. Suryadevara

Tata Institute of Fundamental Research-B, Mumbai, India
A. Bala, S. Banerjee, R.M. Chatterjee, M. Guchait, S. Karmakar, S. Kumar, G. Majumder, K. Mazumdar, S. Mukherjee, A. Thachayath

National Institute of Science Education and Research, An OCC of Homi Bhabha National Institute, Bhubaneswar, Odisha, India
S. Bahinipati[40], A.K. Das, C. Kar, D. Maity[41], P. Mal, T. Mishra, V.K. Muraleedharan Nair Bindhu[41], K. Naskar[41], A. Nayak[41], P. Sadangi, P. Saha, S.K. Swain, S. Varghese[41], D. Vats[41]

Indian Institute of Science Education and Research (IISER), Pune, India
A. Alpana, S. Dube, B. Kansal, A. Laha, A. Rastogi, S. Sharma

Isfahan University of Technology, Isfahan, Iran
H. Bakhshiansohi[42], E. Khazaie[43], M. Zeinali[44]

Institute for Research in Fundamental Sciences (IPM), Tehran, Iran
S. Chenarani[45], S.M. Etesami, M. Khakzad, M. Mohammadi Najafabadi

University College Dublin, Dublin, Ireland
M. Grunewald

INFN Sezione di Bari[a], Università di Bari[b], Politecnico di Bari[c], Bari, Italy
M. Abbrescia[a,b], R. Aly[a,c,46], A. Colaleo[a,b], D. Creanza[a,c], B. D'Anzi[a,b], N. De Filippis[a,c], M. De Palma[a,b], A. Di Florio[a,c], W. Elmetenawee[a,b,46], L. Fiore[a], G. Iaselli[a,c], G. Maggi[a,c], M. Maggi[a], I. Margjeka[a,b], V. Mastrapasqua[a,b], S. My[a,b], S. Nuzzo[a,b], A. Pellecchia[a,b], A. Pompili[a,b], G. Pugliese[a,c], R. Radogna[a], G. Ramirez-Sanchez[a,c], D. Ramos[a], A. Ranieri[a], L. Silvestris[a], F.M. Simone[a,b], Ü. Sözbilir[a], A. Stamerra[a], R. Venditti[a], P. Verwilligen[a], A. Zaza[a,b]

INFN Sezione di Bologna[a], Università di Bologna[b], Bologna, Italy
G. Abbiendi[a], C. Battilana[a,b], D. Bonacorsi[a,b], L. Borgonovi[a], R. Campanini[a,b], P. Capiluppi[a,b], A. Castro[a,b], F.R. Cavallo[a], M. Cuffiani[a,b], G.M. Dallavalle[a], T. Diotalevi[a,b], F. Fabbri[a], A. Fanfani[a,b], D. Fasanella[a,b], P. Giacomelli[a], L. Giommi[a,b], C. Grandi[a], L. Guiducci[a,b], S. Lo Meo[a,47], L. Lunerti[a,b], S. Marcellini[a], G. Masetti[a], F.L. Navarria[a,b], F. Primavera[a,b], A.M. Rossi[a,b], T. Rovelli[a,b], G.P. Siroli[a,b]

INFN Sezione di Catania[a], Università di Catania[b], Catania, Italy
S. Costa[a,b,48], A. Di Mattia[a], R. Potenza[a,b], A. Tricomi[a,b,48], C. Tuve[a,b]

INFN Sezione di Firenze[a], Università di Firenze[b], Firenze, Italy
G. Barbagli[a], G. Bardelli[a,b], B. Camaiani[a,b], A. Cassese[a], R. Ceccarelli[a], V. Ciulli[a,b], C. Civinini[a], R. D'Alessandro[a,b], E. Focardi[a,b], G. Latino[a,b], P. Lenzi[a,b], M. Lizzo[a], M. Meschini[a], S. Paoletti[a], A. Papanastassiou[a,b], G. Sguazzoni[a], L. Viliani[a]

INFN Laboratori Nazionali di Frascati, Frascati, Italy
L. Benussi, S. Bianco, S. Meola[49], D. Piccolo

INFN Sezione di Genova[a], Università di Genova[b], Genova, Italy
P. Chatagnon[a], F. Ferro[a], E. Robutti[a], S. Tosi[a,b]

INFN Sezione di Milano-Bicocca[a], Università di Milano-Bicocca[b], Milano, Italy
A. Benaglia[a], G. Boldrini[a], F. Brivio[a], F. Cetorelli[a], F. De Guio[a,b], M.E. Dinardo[a,b], P. Dini[a], S. Gennai[a], A. Ghezzi[a,b], P. Govoni[a,b], L. Guzzi[a], M.T. Lucchini[a,b], M. Malberti[a], S. Malvezzi[a], A. Massironi[a], D. Menasce[a], L. Moroni[a], M. Paganoni[a,b], D. Pedrini[a], B.S. Pinolini[a], S. Ragazzi[a,b], N. Redaelli[a],

T. Tabarelli de Fatis[a,b], D. Zuolo[a]

INFN Sezione di Napoli[a], Università di Napoli 'Federico II'[b], Napoli, Italy; Università della Basilicata[c], Potenza, Italy; Università G. Marconi[d], Roma, Italy
S. Buontempo[a], A. Cagnotta[a,b], F. Carnevali[a,b], N. Cavallo[a,c], A. De Iorio[a,b], F. Fabozzi[a,c], A.O.M. Iorio[a,b], L. Lista[a,b,50], P. Paolucci[a,28], B. Rossi[a], C. Sciacca[a,b]

INFN Sezione di Padova[a], Università di Padova[b], Padova, Italy; Università di Trento[c], Trento, Italy
R. Ardino[a], P. Azzi[a], N. Bacchetta[a,51], M. Biasotto[a,52], D. Bisello[a,b], P. Bortignon[a], A. Bragagnolo[a,b], P. Checchia[a], T. Dorigo[a], S. Fantinel[a], F. Gasparini[a,b], U. Gasparini[a,b], G. Grosso[a], L. Layer[a,53], E. Lusiani[a], M. Margoni[a,b], M. Migliorini[a,b], J. Pazzini[a,b], P. Ronchese[a,b], R. Rossin[a,b], F. Simonetto[a,b], G. Strong[a], M. Tosi[a,b], A. Triossi[a,b], S. Ventura[a], H. Yarar[a,b], M. Zanetti[a,b], P. Zotto[a,b], A. Zucchetta[a,b], G. Zumerle[a,b]

INFN Sezione di Pavia[a], Università di Pavia[b], Pavia, Italy
S. Abu Zeid[a,54], C. Aimè[a,b], A. Braghieri[a], S. Calzaferri[a,b], D. Fiorina[a,b], P. Montagna[a,b], V. Re[a], C. Riccardi[a,b], P. Salvini[a], I. Vai[a,b], P. Vitulo[a,b]

INFN Sezione di Perugia[a], Università di Perugia[b], Perugia, Italy
S. Ajmal[a,b], P. Asenov[a,55], G.M. Bilei[a], D. Ciangottini[a,b], L. Fanò[a,b], M. Magherini[a,b], G. Mantovani[a,b], V. Mariani[a,b], M. Menichelli[a], F. Moscatelli[a,55], A. Piccinelli[a,b], M. Presilla[a,b], A. Rossi[a,b], A. Santocchia[a,b], D. Spiga[a], T. Tedeschi[a,b]

INFN Sezione di Pisa[a], Università di Pisa[b], Scuola Normale Superiore di Pisa[c], Pisa, Italy; Università di Siena[d], Siena, Italy
P. Azzurri[a], G. Bagliesi[a], R. Bhattacharya[a], L. Bianchini[a,b], T. Boccali[a], E. Bossini[a], D. Bruschini[a,c], R. Castaldi[a], M.A. Ciocci[a,b], M. Cipriani[a,b], V. D'Amante[a,d], R. Dell'Orso[a], S. Donato[a], A. Giassi[a], F. Ligabue[a,c], D. Matos Figueiredo[a], A. Messineo[a,b], M. Musich[a,b], F. Palla[a], S. Parolia[a], A. Rizzi[a,b], G. Rolandi[a,c], S. Roy Chowdhury[a], T. Sarkar[a], A. Scribano[a], P. Spagnolo[a], R. Tenchini[a,b], G. Tonelli[a,b], N. Turini[a,d], A. Venturi[a], P.G. Verdini[a]

INFN Sezione di Roma[a], Sapienza Università di Roma[b], Roma, Italy
P. Barria[a], M. Campana[a,b], F. Cavallari[a], L. Cunqueiro Mendez[a,b], D. Del Re[a,b], E. Di Marco[a], M. Diemoz[a], F. Errico[a,b], E. Longo[a,b], P. Meridiani[a], J. Mijuskovic[a,b], G. Organtini[a,b], F. Pandolfi[a], R. Paramatti[a,b], C. Quaranta[a,b], S. Rahatlou[a,b], C. Rovelli[a], F. Santanastasio[a,b], L. Soffi[a], R. Tramontano[a,b]

INFN Sezione di Torino[a], Università di Torino[b], Torino, Italy; Università del Piemonte Orientale[c], Novara, Italy
N. Amapane[a,b], R. Arcidiacono[a,c], S. Argiro[a,b], M. Arneodo[a,c], N. Bartosik[a], R. Bellan[a,b], A. Bellora[a,b], C. Biino[a], N. Cartiglia[a], M. Costa[a,b], R. Covarelli[a,b], N. Demaria[a], L. Finco[a], M. Grippo[a,b], B. Kiani[a,b], F. Legger[a], F. Luongo[a,b], C. Mariotti[a], S. Maselli[a], A. Mecca[a,b], E. Migliore[a,b], M. Monteno[a], R. Mulargia[a], M.M. Obertino[a,b], G. Ortona[a], L. Pacher[a,b], N. Pastrone[a], M. Pelliccioni[a], M. Ruspa[a,c], F. Siviero[a,b], V. Sola[a,b], A. Solano[a,b], D. Soldi[a,b], A. Staiano[a], C. Tarricone[a,b], M. Tornago[a,b], D. Trocino[a], G. Umoret[a,b], E. Vlasov[a,b]

INFN Sezione di Trieste[a], Università di Trieste[b], Trieste, Italy
S. Belforte[a], V. Candelise[a,b], M. Casarsa[a], F. Cossutti[a], K. De Leo[a,b], G. Della Ricca[a,b]

Kyungpook National University, Daegu, Korea
S. Dogra, J. Hong, C. Huh, B. Kim, D.H. Kim, J. Kim, H. Lee, S.W. Lee, C.S. Moon, Y.D. Oh, S.I. Pak, M.S. Ryu, S. Sekmen, Y.C. Yang

Chonnam National University, Institute for Universe and Elementary Particles, Kwangju, Korea
G. Bak, P. Gwak, H. Kim, D.H. Moon

Hanyang University, Seoul, Korea
E. Asilar, D. Kim, T.J. Kim, J.A. Merlin, J. Park

Korea University, Seoul, Korea
S. Choi, S. Han, B. Hong, K. Lee, K.S. Lee, S. Lee, J. Park, S.K. Park, J. Yoo

Kyung Hee University, Department of Physics, Seoul, Korea
J. Goh

Sejong University, Seoul, Korea
H. S. Kim, Y. Kim, S. Lee

Seoul National University, Seoul, Korea
J. Almond, J.H. Bhyun, J. Choi, S. Jeon, W. Jun, J. Kim, J.S. Kim, S. Ko, H. Kwon, H. Lee, J. Lee, J. Lee, S. Lee, B.H. Oh, S.B. Oh, H. Seo, U.K. Yang, I. Yoon

University of Seoul, Seoul, Korea
W. Jang, D.Y. Kang, Y. Kang, S. Kim, B. Ko, J.S.H. Lee, Y. Lee, I.C. Park, Y. Roh, I.J. Watson, S. Yang

Yonsei University, Department of Physics, Seoul, Korea
S. Ha, H.D. Yoo

Sungkyunkwan University, Suwon, Korea
M. Choi, M.R. Kim, H. Lee, Y. Lee, I. Yu

College of Engineering and Technology, American University of the Middle East (AUM), Dasman, Kuwait
T. Beyrouthy, Y. Maghrbi

Riga Technical University, Riga, Latvia
K. Dreimanis, A. Gaile, G. Pikurs, A. Potrebko, M. Seidel, V. Veckalns[56]

University of Latvia (LU), Riga, Latvia
N.R. Strautnieks

Vilnius University, Vilnius, Lithuania
M. Ambrozas, A. Juodagalvis, A. Rinkevicius, G. Tamulaitis

National Centre for Particle Physics, Universiti Malaya, Kuala Lumpur, Malaysia
N. Bin Norjoharuddeen, I. Yusuff[57], Z. Zolkapli

Universidad de Sonora (UNISON), Hermosillo, Mexico
J.F. Benitez, A. Castaneda Hernandez, H.A. Encinas Acosta, L.G. Gallegos Maríñez, M. León Coello, J.A. Murillo Quijada, A. Sehrawat, L. Valencia Palomo

Centro de Investigacion y de Estudios Avanzados del IPN, Mexico City, Mexico
G. Ayala, H. Castilla-Valdez, E. De La Cruz-Burelo, I. Heredia-De La Cruz[58], R. Lopez-Fernandez, C.A. Mondragon Herrera, A. Sánchez Hernández

Universidad Iberoamericana, Mexico City, Mexico
C. Oropeza Barrera, M. Ramírez García

Benemerita Universidad Autonoma de Puebla, Puebla, Mexico
I. Bautista, I. Pedraza, H.A. Salazar Ibarguen, C. Uribe Estrada

University of Montenegro, Podgorica, Montenegro
I. Bubanja, N. Raicevic

University of Canterbury, Christchurch, New Zealand
P.H. Butler

National Centre for Physics, Quaid-I-Azam University, Islamabad, Pakistan
A. Ahmad, M.I. Asghar, A. Awais, M.I.M. Awan, H.R. Hoorani, W.A. Khan

AGH University of Krakow, Faculty of Computer Science, Electronics and Telecommunications, Krakow, Poland
V. Avati, L. Grzanka, M. Malawski

National Centre for Nuclear Research, Swierk, Poland
H. Bialkowska, M. Bluj, B. Boimska, M. Górski, M. Kazana, M. Szleper, P. Zalewski

Institute of Experimental Physics, Faculty of Physics, University of Warsaw, Warsaw, Poland
K. Bunkowski, K. Doroba, A. Kalinowski, M. Konecki, J. Krolikowski, A. Muhammad

Warsaw University of Technology, Warsaw, Poland
K. Pozniak, W. Zabolotny

Laboratório de Instrumentação e Física Experimental de Partículas, Lisboa, Portugal
M. Araujo, D. Bastos, C. Beirão Da Cruz E Silva, A. Boletti, M. Bozzo, P. Faccioli, M. Gallinaro, J. Hollar, N. Leonardo, T. Niknejad, A. Petrilli, M. Pisano, J. Seixas, J. Varela

Faculty of Physics, University of Belgrade, Belgrade, Serbia
P. Adzic, P. Milenovic

VINCA Institute of Nuclear Sciences, University of Belgrade, Belgrade, Serbia
M. Dordevic, J. Milosevic, V. Rekovic

Centro de Investigaciones Energéticas Medioambientales y Tecnológicas (CIEMAT), Madrid, Spain
M. Aguilar-Benitez, J. Alcaraz Maestre, M. Barrio Luna, Cristina F. Bedoya, M. Cepeda, M. Cerrada, N. Colino, B. De La Cruz, A. Delgado Peris, D. Fernández Del Val, J.P. Fernández Ramos, J. Flix, M.C. Fouz, O. Gonzalez Lopez, S. Goy Lopez, J.M. Hernandez, M.I. Josa, J. León Holgado, D. Moran, C. M. Morcillo Perez, Á. Navarro Tobar, C. Perez Dengra, A. Pérez-Calero Yzquierdo, J. Puerta Pelayo, I. Redondo, D.D. Redondo Ferrero, L. Romero, S. Sánchez Navas, L. Urda Gómez, J. Vazquez Escobar, C. Willmott

Universidad Autónoma de Madrid, Madrid, Spain

J.F. de Trocóniz

Universidad de Oviedo, Instituto Universitario de Ciencias y Tecnologías Espaciales de Asturias (ICTEA), Oviedo, Spain
B. Alvarez Gonzalez, J. Cuevas, J. Fernandez Menendez, S. Folgueras, I. Gonzalez Caballero, J.R. González Fernández, E. Palencia Cortezon, C. Ramón Álvarez, V. Rodríguez Bouza, A. Soto Rodríguez, A. Trapote, C. Vico Villalba, P. Vischia

Instituto de Física de Cantabria (IFCA), CSIC-Universidad de Cantabria, Santander, Spain
S. Bhowmik, S. Blanco Fernández, J.A. Brochero Cifuentes, I.J. Cabrillo, A. Calderon, J. Duarte Campderros, M. Fernandez, C. Fernandez Madrazo, G. Gomez, C. Lasaosa García, C. Martinez Rivero, P. Martinez Ruiz del Arbol, F. Matorras, P. Matorras Cuevas, E. Navarrete Ramos, J. Piedra Gomez, C. Prieels, L. Scodellaro, I. Vila, J.M. Vizan Garcia

University of Colombo, Colombo, Sri Lanka
M.K. Jayananda, B. Kailasapathy[59], D.U.J. Sonnadara, D.D.C. Wickramarathna

University of Ruhuna, Department of Physics, Matara, Sri Lanka
W.G.D. Dharmaratna[60], K. Liyanage, N. Perera, N. Wickramage

CERN, European Organization for Nuclear Research, Geneva, Switzerland
D. Abbaneo, C. Amendola, E. Auffray, G. Auzinger, J. Baechler, D. Barney, A. Bermúdez Martínez, M. Bianco, B. Bilin, A.A. Bin Anuar, A. Bocci, E. Brondolin, C. Caillol, T. Camporesi, G. Cerminara, N. Chernyavskaya, D. d'Enterria, A. Dabrowski, A. David, A. De Roeck, M.M. Defranchis, M. Deile, M. Dobson, F. Fallavollita[61], L. Forthomme, G. Franzoni, W. Funk, S. Giani, D. Gigi, K. Gill, F. Glege, L. Gouskos, M. Haranko, J. Hegeman, V. Innocente, T. James, P. Janot, J. Kieseler, S. Laurila, P. Lecoq, E. Leutgeb, C. Lourenço, B. Maier, L. Malgeri, M. Mannelli, A.C. Marini, F. Meijers, S. Mersi, E. Meschi, V. Milosevic, F. Moortgat, M. Mulders, S. Orfanelli, F. Pantaleo, M. Peruzzi, G. Petrucciani, A. Pfeiffer, M. Pierini, D. Piparo, H. Qu, D. Rabady, G. Reales Gutiérrez, M. Rovere, H. Sakulin, S. Scarfi, M. Selvaggi, A. Sharma, K. Shchelina, P. Silva, P. Sphicas[62], A.G. Stahl Leiton, A. Steen, S. Summers, D. Treille, P. Tropea, A. Tsirou, D. Walter, J. Wanczyk[63], K.A. Wozniak[64], P. Zehetner, P. Zejdl, W.D. Zeuner

Paul Scherrer Institut, Villigen, Switzerland
T. Bevilacqua[65], L. Caminada[65], A. Ebrahimi, W. Erdmann, R. Horisberger, Q. Ingram, H.C. Kaestli, D. Kotlinski, C. Lange, M. Missiroli[65], L. Noehte[65], T. Rohe

ETH Zurich - Institute for Particle Physics and Astrophysics (IPA), Zurich, Switzerland
T.K. Aarrestad, K. Androsov[63], M. Backhaus, A. Calandri, C. Cazzaniga, K. Datta, A. De Cosa, G. Dissertori, M. Dittmar, M. Donegà, F. Eble, M. Galli, K. Gedia, F. Glessgen, C. Grab, D. Hits, W. Lustermann, A.-M. Lyon, R.A. Manzoni, M. Marchegiani, L. Marchese, C. Martin Perez, A. Mascellani[63], F. Nessi-Tedaldi, F. Pauss, V. Perovic, S. Pigazzini, M.G. Ratti, M. Reichmann, C. Reissel, T. Reitenspiess, B. Ristic, F. Riti, D. Ruini, D.A. Sanz Becerra, R. Seidita, J. Steggemann[63], D. Valsecchi, R. Wallny

Universität Zürich, Zurich, Switzerland
C. Amsler[66], P. Bärtschi, C. Botta, D. Brzhechko, M.F. Canelli, K. Cormier,

R. Del Burgo, J.K. Heikkilä, M. Huwiler, W. Jin, A. Jofrehei, B. Kilminster, S. Leontsinis, S.P. Liechti, A. Macchiolo, P. Meiring, V.M. Mikuni, U. Molinatti, I. Neutelings, A. Reimers, P. Robmann, S. Sanchez Cruz, K. Schweiger, M. Senger, Y. Takahashi

National Central University, Chung-Li, Taiwan
C. Adloff[67], C.M. Kuo, W. Lin, P.K. Rout, P.C. Tiwari[39], S.S. Yu

National Taiwan University (NTU), Taipei, Taiwan
L. Ceard, Y. Chao, K.F. Chen, P.s. Chen, Z.g. Chen, W.-S. Hou, T.h. Hsu, Y.w. Kao, R. Khurana, G. Kole, Y.y. Li, R.-S. Lu, E. Paganis, A. Psallidas, X.f. Su, J. Thomas-Wilsker, H.y. Wu, E. Yazgan

High Energy Physics Research Unit, Department of Physics, Faculty of Science, Chulalongkorn University, Bangkok, Thailand
C. Asawatangtrakuldee, N. Srimanobhas, V. Wachirapusitanand

Çukurova University, Physics Department, Science and Art Faculty, Adana, Turkey
D. Agyel, F. Boran, Z.S. Demiroglu, F. Dolek, I. Dumanoglu[68], E. Eskut, Y. Guler[69], E. Gurpinar Guler[69], C. Isik, O. Kara, A. Kayis Topaksu, U. Kiminsu, G. Onengut, K. Ozdemir[70], A. Polatoz, B. Tali[71], U.G. Tok, S. Turkcapar, E. Uslan, I.S. Zorbakir

Middle East Technical University, Physics Department, Ankara, Turkey
K. Ocalan[72], M. Yalvac[73]

Bogazici University, Istanbul, Turkey
B. Akgun, I.O. Atakisi, E. Gülmez, M. Kaya[74], O. Kaya[75], S. Tekten[76]

Istanbul Technical University, Istanbul, Turkey
A. Cakir, K. Cankocak[68], Y. Komurcu, S. Sen[77]

Istanbul University, Istanbul, Turkey
O. Aydilek, S. Cerci[71], V. Epshteyn, B. Hacisahinoglu, I. Hos[78], B. Isildak[79], B. Kaynak, S. Ozkorucuklu, O. Potok, H. Sert, C. Simsek, D. Sunar Cerci[71], C. Zorbilmez

Institute for Scintillation Materials of National Academy of Science of Ukraine, Kharkiv, Ukraine
A. Boyaryntsev, B. Grynyov

National Science Centre, Kharkiv Institute of Physics and Technology, Kharkiv, Ukraine
L. Levchuk

University of Bristol, Bristol, United Kingdom
D. Anthony, J.J. Brooke, A. Bundock, F. Bury, E. Clement, D. Cussans, H. Flacher, M. Glowacki, J. Goldstein, H.F. Heath, L. Kreczko, B. Krikler, S. Paramesvaran, S. Seif El Nasr-Storey, V.J. Smith, N. Stylianou[80], K. Walkingshaw Pass, R. White

Rutherford Appleton Laboratory, Didcot, United Kingdom
A.H. Ball, K.W. Bell, A. Belyaev[81], C. Brew, R.M. Brown, D.J.A. Cockerill, C. Cooke, K.V. Ellis, K. Harder, S. Harper, M.-L. Holmberg[82], Sh. Jain, J. Linacre, K. Manolopoulos, D.M. Newbold, E. Olaiya, D. Petyt, T. Reis, G. Salvi, T. Schuh, C.H. Shepherd-Themistocleous, I.R. Tomalin, T. Williams

Imperial College, London, United Kingdom
R. Bainbridge, P. Bloch, C.E. Brown, O. Buchmuller, V. Cacchio, C.A. Carrillo Montoya, G.S. Chahal[83], D. Colling, J.S. Dancu, P. Dauncey, G. Davies, J. Davies, M. Della Negra, S. Fayer, G. Fedi, G. Hall, M.H. Hassanshahi, A. Howard, G. Iles, M. Knight, J. Langford, L. Lyons, A.-M. Magnan, S. Malik, A. Martelli, M. Mieskolainen, J. Nash[84], M. Pesaresi, B.C. Radburn-Smith, A. Richards, A. Rose, C. Seez, R. Shukla, A. Tapper, K. Uchida, G.P. Uttley, L.H. Vage, T. Virdee[28], M. Vojinovic, N. Wardle, D. Winterbottom

Brunel University, Uxbridge, United Kingdom
K. Coldham, J.E. Cole, A. Khan, P. Kyberd, I.D. Reid

Baylor University, Waco, Texas, USA
S. Abdullin, A. Brinkerhoff, B. Caraway, J. Dittmann, K. Hatakeyama, J. Hiltbrand, A.R. Kanuganti, B. McMaster, M. Saunders, S. Sawant, C. Sutantawibul, M. Toms[85], J. Wilson

Catholic University of America, Washington, DC, USA
R. Bartek, A. Dominguez, C. Huerta Escamilla, A.E. Simsek, R. Uniyal, A.M. Vargas Hernandez

The University of Alabama, Tuscaloosa, Alabama, USA
R. Chudasama, S.I. Cooper, S.V. Gleyzer, C.U. Perez, P. Rumerio[86], E. Usai, C. West, R. Yi

Boston University, Boston, Massachusetts, USA
A. Akpinar, A. Albert, D. Arcaro, C. Cosby, Z. Demiragli, C. Erice, E. Fontanesi, D. Gastler, J. Rohlf, K. Salyer, D. Sperka, D. Spitzbart, I. Suarez, A. Tsatsos, S. Yuan

Brown University, Providence, Rhode Island, USA
G. Benelli, X. Coubez[23], D. Cutts, M. Hadley, U. Heintz, J.M. Hogan[87], T. Kwon, G. Landsberg, K.T. Lau, D. Li, J. Luo, S. Mondal, M. Narain[†], N. Pervan, S. Sagir[88], F. Simpson, M. Stamenkovic, W.Y. Wong, X. Yan, W. Zhang

University of California, Davis, Davis, California, USA
S. Abbott, J. Bonilla, C. Brainerd, R. Breedon, M. Calderon De La Barca Sanchez, M. Chertok, M. Citron, J. Conway, P.T. Cox, R. Erbacher, G. Haza, F. Jensen, O. Kukral, G. Mocellin, M. Mulhearn, D. Pellett, B. Regnery, W. Wei, Y. Yao, F. Zhang

University of California, Los Angeles, California, USA
M. Bachtis, R. Cousins, A. Datta, J. Hauser, M. Ignatenko, M.A. Iqbal, T. Lam, E. Manca, W.A. Nash, D. Saltzberg, B. Stone, V. Valuev

University of California, Riverside, Riverside, California, USA
R. Clare, M. Gordon, G. Hanson, W. Si, S. Wimpenny[†]

University of California, San Diego, La Jolla, California, USA
J.G. Branson, S. Cittolin, S. Cooperstein, D. Diaz, J. Duarte, R. Gerosa, L. Giannini, J. Guiang, R. Kansal, V. Krutelyov, R. Lee, J. Letts, M. Masciovecchio, F. Mokhtar, M. Pieri, M. Quinnan, B.V. Sathia Narayanan, V. Sharma, M. Tadel, E. Vourliotis, F. Würthwein, Y. Xiang, A. Yagil

University of California, Santa Barbara - Department of Physics, Santa Barbara, California,

USA
A. Barzdukas, L. Brennan, C. Campagnari, G. Collura, A. Dorsett, J. Incandela, M. Kilpatrick, J. Kim, A.J. Li, P. Masterson, H. Mei, M. Oshiro, J. Richman, U. Sarica, R. Schmitz, F. Setti, J. Sheplock, D. Stuart, S. Wang

California Institute of Technology, Pasadena, California, USA
A. Bornheim, O. Cerri, A. Latorre, J.M. Lawhorn, J. Mao, H.B. Newman, T. Q. Nguyen, M. Spiropulu, J.R. Vlimant, C. Wang, S. Xie, R.Y. Zhu

Carnegie Mellon University, Pittsburgh, Pennsylvania, USA
J. Alison, S. An, M.B. Andrews, P. Bryant, V. Dutta, T. Ferguson, A. Harilal, C. Liu, T. Mudholkar, S. Murthy, M. Paulini, A. Roberts, A. Sanchez, W. Terrill

University of Colorado Boulder, Boulder, Colorado, USA
J.P. Cumalat, W.T. Ford, A. Hassani, G. Karathanasis, E. MacDonald, N. Manganelli, F. Marini, A. Perloff, C. Savard, N. Schonbeck, K. Stenson, K.A. Ulmer, S.R. Wagner, N. Zipper

Cornell University, Ithaca, New York, USA
J. Alexander, S. Bright-Thonney, X. Chen, D.J. Cranshaw, J. Fan, X. Fan, D. Gadkari, S. Hogan, J. Monroy, J.R. Patterson, J. Reichert, M. Reid, A. Ryd, J. Thom, P. Wittich, R. Zou

Fermi National Accelerator Laboratory, Batavia, Illinois, USA
M. Albrow, M. Alyari, O. Amram, G. Apollinari, A. Apresyan, L.A.T. Bauerdick, D. Berry, J. Berryhill, P.C. Bhat, K. Burkett, J.N. Butler, A. Canepa, G.B. Cerati, H.W.K. Cheung, F. Chlebana, G. Cummings, J. Dickinson, I. Dutta, V.D. Elvira, Y. Feng, J. Freeman, A. Gandrakota, Z. Gecse, L. Gray, D. Green, S. Grünendahl, D. Guerrero, O. Gutsche, R.M. Harris, R. Heller, T.C. Herwig, J. Hirschauer, L. Horyn, B. Jayatilaka, S. Jindariani, M. Johnson, U. Joshi, T. Klijnsma, B. Klima, K.H.M. Kwok, S. Lammel, D. Lincoln, R. Lipton, T. Liu, C. Madrid, K. Maeshima, C. Mantilla, D. Mason, P. McBride, P. Merkel, S. Mrenna, S. Nahn, J. Ngadiuba, D. Noonan, V. Papadimitriou, N. Pastika, K. Pedro, C. Pena[89], F. Ravera, A. Reinsvold Hall[90], L. Ristori, E. Sexton-Kennedy, N. Smith, A. Soha, L. Spiegel, S. Stoynev, J. Strait, L. Taylor, S. Tkaczyk, N.V. Tran, L. Uplegger, E.W. Vaandering, I. Zoi

University of Florida, Gainesville, Florida, USA
C. Aruta, P. Avery, D. Bourilkov, L. Cadamuro, P. Chang, V. Cherepanov, R.D. Field, E. Koenig, M. Kolosova, J. Konigsberg, A. Korytov, K.H. Lo, K. Matchev, N. Menendez, G. Mitselmakher, A. Muthirakalayil Madhu, N. Rawal, D. Rosenzweig, S. Rosenzweig, K. Shi, J. Wang

Florida State University, Tallahassee, Florida, USA
T. Adams, A. Al Kadhim, A. Askew, N. Bower, R. Habibullah, V. Hagopian, R. Hashmi, R.S. Kim, S. Kim, T. Kolberg, G. Martinez, H. Prosper, P.R. Prova, O. Viazlo, M. Wulansatiti, R. Yohay, J. Zhang

Florida Institute of Technology, Melbourne, Florida, USA
B. Alsufyani, M.M. Baarmand, S. Butalla, T. Elkafrawy[54], M. Hohlmann, R. Kumar Verma, M. Rahmani

University of Illinois Chicago, Chicago, USA, Chicago, USA
M.R. Adams, C. Bennett, R. Cavanaugh, S. Dittmer, R. Escobar Franco, O. Evdoki-

mov, C.E. Gerber, D.J. Hofman, J.h. Lee, D. S. Lemos, A.H. Merrit, C. Mills, S. Nanda, G. Oh, B. Ozek, D. Pilipovic, T. Roy, S. Rudrabhatla, M.B. Tonjes, N. Varelas, X. Wang, Z. Ye, J. Yoo

The University of Iowa, Iowa City, Iowa, USA
M. Alhusseini, D. Blend, K. Dilsiz[91], L. Emediato, G. Karaman, O.K. Köseyan, J.-P. Merlo, A. Mestvirishvili[92], J. Nachtman, O. Neogi, H. Ogul[93], Y. Onel, A. Penzo, C. Snyder, E. Tiras[94]

Johns Hopkins University, Baltimore, Maryland, USA
B. Blumenfeld, L. Corcodilos, J. Davis, A.V. Gritsan, L. Kang, S. Kyriacou, P. Maksimovic, M. Roguljic, J. Roskes, S. Sekhar, M. Swartz, T.Á. Vámi

The University of Kansas, Lawrence, Kansas, USA
A. Abreu, L.F. Alcerro Alcerro, J. Anguiano, P. Baringer, A. Bean, Z. Flowers, D. Grove, J. King, G. Krintiras, M. Lazarovits, C. Le Mahieu, C. Lindsey, J. Marquez, N. Minafra, M. Murray, M. Nickel, M. Pitt, S. Popescu[95], C. Rogan, C. Royon, R. Salvatico, S. Sanders, C. Smith, Q. Wang, G. Wilson

Kansas State University, Manhattan, Kansas, USA
B. Allmond, A. Ivanov, K. Kaadze, A. Kalogeropoulos, D. Kim, Y. Maravin, K. Nam, J. Natoli, D. Roy, G. Sorrentino

Lawrence Livermore National Laboratory, Livermore, California, USA
F. Rebassoo, D. Wright

University of Maryland, College Park, Maryland, USA
E. Adams, A. Baden, O. Baron, A. Belloni, A. Bethani, Y.M. Chen, S.C. Eno, N.J. Hadley, S. Jabeen, R.G. Kellogg, T. Koeth, Y. Lai, S. Lascio, A.C. Mignerey, S. Nabili, C. Palmer, C. Papageorgakis, M.M. Paranjpe, L. Wang, K. Wong

Massachusetts Institute of Technology, Cambridge, Massachusetts, USA
J. Bendavid, W. Busza, I.A. Cali, Y. Chen, M. D'Alfonso, J. Eysermans, C. Freer, G. Gomez-Ceballos, M. Goncharov, P. Harris, D. Hoang, D. Kovalskyi, J. Krupa, L. Lavezzo, Y.-J. Lee, K. Long, C. Mironov, C. Paus, D. Rankin, C. Roland, G. Roland, S. Rothman, Z. Shi, G.S.F. Stephans, J. Wang, Z. Wang, B. Wyslouch, T. J. Yang

University of Minnesota, Minneapolis, Minnesota, USA
B. Crossman, B.M. Joshi, C. Kapsiak, M. Krohn, D. Mahon, J. Mans, B. Marzocchi, S. Pandey, M. Revering, R. Rusack, R. Saradhy, N. Schroeder, N. Strobbe, M.A. Wadud

University of Mississippi, Oxford, Mississippi, USA
L.M. Cremaldi

University of Nebraska-Lincoln, Lincoln, Nebraska, USA
K. Bloom, M. Bryson, D.R. Claes, C. Fangmeier, F. Golf, J. Hossain, C. Joo, I. Kravchenko, I. Reed, J.E. Siado, G.R. Snow†, W. Tabb, A. Vagnerini, A. Wightman, F. Yan, D. Yu, A.G. Zecchinelli

State University of New York at Buffalo, Buffalo, New York, USA
G. Agarwal, H. Bandyopadhyay, L. Hay, I. Iashvili, A. Kharchilava, C. McLean, M. Morris, D. Nguyen, J. Pekkanen, S. Rappoccio, H. Rejeb Sfar, A. Williams

Northeastern University, Boston, Massachusetts, USA
G. Alverson, E. Barberis, Y. Haddad, Y. Han, A. Krishna, J. Li, M. Lu, G. Madigan, D.M. Morse, V. Nguyen, T. Orimoto, A. Parker, L. Skinnari, A. Tishelman-Charny, B. Wang, D. Wood

Northwestern University, Evanston, Illinois, USA
S. Bhattacharya, J. Bueghly, Z. Chen, K.A. Hahn, Y. Liu, Y. Miao, D.G. Monk, M.H. Schmitt, A. Taliercio, M. Velasco

University of Notre Dame, Notre Dame, Indiana, USA
R. Band, R. Bucci, S. Castells, M. Cremonesi, A. Das, R. Goldouzian, M. Hildreth, K.W. Ho, K. Hurtado Anampa, C. Jessop, K. Lannon, J. Lawrence, N. Loukas, L. Lutton, J. Mariano, N. Marinelli, I. Mcalister, T. McCauley, C. Mcgrady, K. Mohrman, C. Moore, Y. Musienko[12], H. Nelson, M. Osherson, R. Ruchti, A. Townsend, M. Wayne, H. Yockey, M. Zarucki, L. Zygala

The Ohio State University, Columbus, Ohio, USA
A. Basnet, B. Bylsma, M. Carrigan, L.S. Durkin, C. Hill, M. Joyce, A. Lesauvage, M. Nunez Ornelas, K. Wei, B.L. Winer, B. R. Yates

Princeton University, Princeton, New Jersey, USA
F.M. Addesa, H. Bouchamaoui, P. Das, G. Dezoort, P. Elmer, A. Frankenthal, B. Greenberg, N. Haubrich, S. Higginbotham, G. Kopp, S. Kwan, D. Lange, A. Loeliger, D. Marlow, I. Ojalvo, J. Olsen, D. Stickland, C. Tully

University of Puerto Rico, Mayaguez, Puerto Rico, USA
S. Malik

Purdue University, West Lafayette, Indiana, USA
A.S. Bakshi, V.E. Barnes, S. Chandra, R. Chawla, S. Das, A. Gu, L. Gutay, M. Jones, A.W. Jung, D. Kondratyev, A.M. Koshy, M. Liu, G. Negro, N. Neumeister, G. Paspalaki, S. Piperov, A. Purohit, J.F. Schulte, M. Stojanovic, J. Thieman, A. K. Virdi, F. Wang, W. Xie

Purdue University Northwest, Hammond, Indiana, USA
J. Dolen, N. Parashar, A. Pathak

Rice University, Houston, Texas, USA
D. Acosta, A. Baty, T. Carnahan, S. Dildick, K.M. Ecklund, P.J. Fernández Manteca, S. Freed, P. Gardner, F.J.M. Geurts, A. Kumar, W. Li, O. Miguel Colin, B.P. Padley, R. Redjimi, J. Rotter, E. Yigitbasi, Y. Zhang

University of Rochester, Rochester, New York, USA
A. Bodek, P. de Barbaro, R. Demina, J.L. Dulemba, C. Fallon, A. Garcia-Bellido, O. Hindrichs, A. Khukhunaishvili, P. Parygin[85], E. Popova[85], R. Taus, G.P. Van Onsem

The Rockefeller University, New York, New York, USA
K. Goulianos

Rutgers, The State University of New Jersey, Piscataway, New Jersey, USA
B. Chiarito, J.P. Chou, Y. Gershtein, E. Halkiadakis, A. Hart, M. Heindl, D. Jaroslawski, O. Karacheban[26], I. Laflotte, A. Lath, R. Montalvo, K. Nash, H. Routray, S. Salur, S. Schnetzer, S. Somalwar, R. Stone, S.A. Thayil, S. Thomas, J. Vora, H. Wang

University of Tennessee, Knoxville, Tennessee, USA
H. Acharya, D. Ally, A.G. Delannoy, S. Fiorendi, T. Holmes, N. Karunarathna, L. Lee, E. Nibigira, S. Spanier

Texas A&M University, College Station, Texas, USA
D. Aebi, M. Ahmad, O. Bouhali[96], M. Dalchenko, R. Eusebi, J. Gilmore, T. Huang, T. Kamon[97], H. Kim, S. Luo, S. Malhotra, R. Mueller, D. Overton, D. Rathjens, A. Safonov

Texas Tech University, Lubbock, Texas, USA
N. Akchurin, J. Damgov, V. Hegde, A. Hussain, Y. Kazhykarim, K. Lamichhane, S.W. Lee, A. Mankel, T. Mengke, S. Muthumuni, T. Peltola, I. Volobouev, A. Whitbeck

Vanderbilt University, Nashville, Tennessee, USA
E. Appelt, S. Greene, A. Gurrola, W. Johns, R. Kunnawalkam Elayavalli, A. Melo, F. Romeo, P. Sheldon, S. Tuo, J. Velkovska, J. Viinikainen

University of Virginia, Charlottesville, Virginia, USA
B. Cardwell, B. Cox, J. Hakala, R. Hirosky, A. Ledovskoy, A. Li, C. Neu, C.E. Perez Lara

Wayne State University, Detroit, Michigan, USA
P.E. Karchin

University of Wisconsin - Madison, Madison, Wisconsin, USA
A. Aravind, S. Banerjee, K. Black, T. Bose, S. Dasu, I. De Bruyn, P. Everaerts, C. Galloni, H. He, M. Herndon, A. Herve, C.K. Koraka, A. Lanaro, R. Loveless, J. Madhusudanan Sreekala, A. Mallampalli, A. Mohammadi, S. Mondal, G. Parida, D. Pinna, A. Savin, V. Shang, V. Sharma, W.H. Smith, D. Teague, H.F. Tsoi, W. Vetens, A. Warden

Authors affiliated with an institute or an international laboratory covered by a cooperation agreement with CERN
S. Afanasiev, V. Andreev, Yu. Andreev, T. Aushev, M. Azarkin, A. Babaev, A. Belyaev, V. Blinov[98], E. Boos, V. Borshch, D. Budkouski, V. Bunichev, M. Chadeeva[98], V. Chekhovsky, A. Dermenev, T. Dimova[98], D. Druzhkin[99], M. Dubinin[89], L. Dudko, A. Ershov, G. Gavrilov, V. Gavrilov, S. Gninenko, V. Golovtcov, N. Golubev, I. Golutvin, I. Gorbunov, A. Gribushin, Y. Ivanov, V. Kachanov, L. Kardapoltsev[98], V. Karjavine, A. Karneyeu, V. Kim[98], M. Kirakosyan, D. Kirpichnikov, M. Kirsanov, V. Klyukhin, O. Kodolova[100], D. Konstantinov, V. Korenkov, A. Kozyrev[98], N. Krasnikov, A. Lanev, P. Levchenko[101], N. Lychkovskaya, V. Makarenko, A. Malakhov, V. Matveev[98], V. Murzin, A. Nikitenko[102,100], S. Obraztsov, V. Oreshkin, V. Palichik, V. Perelygin, M. Perfilov, S. Polikarpov[98], V. Popov, O. Radchenko[98], V. Rusinov, M. Savina, V. Savrin, D. Selivanova, V. Shalaev, S. Shmatov, S. Shulha, Y. Skovpen[98], S. Slabospitskii, V. Smirnov, D. Sosnov, V. Sulimov, E. Tcherniaev, A. Terkulov, O. Teryaev, I. Tlisova, A. Toropin, L. Uvarov, A. Uzunian, P. Volkov, A. Vorobyev†, N. Voytishin, B.S. Yuldashev[103], A. Zarubin, I. Zhizhin, A. Zhokin

†: Deceased
[1]Also at Yerevan State University, Yerevan, Armenia
[2]Also at TU Wien, Vienna, Austria

[3]Also at Institute of Basic and Applied Sciences, Faculty of Engineering, Arab Academy for Science, Technology and Maritime Transport, Alexandria, Egypt
[4]Also at Ghent University, Ghent, Belgium
[5]Also at Universidade Estadual de Campinas, Campinas, Brazil
[6]Also at Federal University of Rio Grande do Sul, Porto Alegre, Brazil
[7]Also at UFMS, Nova Andradina, Brazil
[8]Also at Nanjing Normal University, Nanjing, China
[9]Now at The University of Iowa, Iowa City, Iowa, USA
[10]Also at University of Chinese Academy of Sciences, Beijing, China
[11]Also at University of Chinese Academy of Sciences, Beijing, China
[12]Also at an institute or an international laboratory covered by a cooperation agreement with CERN
[13]Also at Suez University, Suez, Egypt
[14]Now at British University in Egypt, Cairo, Egypt
[15]Also at Birla Institute of Technology, Mesra, Mesra, India
[16]Also at Purdue University, West Lafayette, Indiana, USA
[17]Also at Université de Haute Alsace, Mulhouse, France
[18]Also at Department of Physics, Tsinghua University, Beijing, China
[19]Also at Tbilisi State University, Tbilisi, Georgia
[20]Also at The University of the State of Amazonas, Manaus, Brazil
[21]Also at Erzincan Binali Yildirim University, Erzincan, Turkey
[22]Also at University of Hamburg, Hamburg, Germany
[23]Also at RWTH Aachen University, III. Physikalisches Institut A, Aachen, Germany
[24]Also at Isfahan University of Technology, Isfahan, Iran
[25]Also at Bergische University Wuppertal (BUW), Wuppertal, Germany
[26]Also at Brandenburg University of Technology, Cottbus, Germany
[27]Also at Forschungszentrum Jülich, Juelich, Germany
[28]Also at CERN, European Organization for Nuclear Research, Geneva, Switzerland
[29]Also at Institute of Physics, University of Debrecen, Debrecen, Hungary
[30]Also at Institute of Nuclear Research ATOMKI, Debrecen, Hungary
[31]Now at Universitatea Babes-Bolyai - Facultatea de Fizica, Cluj-Napoca, Romania
[32]Also at Physics Department, Faculty of Science, Assiut University, Assiut, Egypt
[33]Also at HUN-REN Wigner Research Centre for Physics, Budapest, Hungary
[34]Also at Faculty of Informatics, University of Debrecen, Debrecen, Hungary
[35]Also at Punjab Agricultural University, Ludhiana, India
[36]Also at UPES - University of Petroleum and Energy Studies, Dehradun, India
[37]Also at University of Visva-Bharati, Santiniketan, India
[38]Also at University of Hyderabad, Hyderabad, India
[39]Also at Indian Institute of Science (IISc), Bangalore, India
[40]Also at IIT Bhubaneswar, Bhubaneswar, India
[41]Also at Institute of Physics, Bhubaneswar, India
[42]Also at Deutsches Elektronen-Synchrotron, Hamburg, Germany
[43]Also at Department of Physics, Isfahan University of Technology, Isfahan, Iran
[44]Also at Sharif University of Technology, Tehran, Iran
[45]Also at Department of Physics, University of Science and Technology of Mazandaran, Behshahr, Iran
[46]Also at Helwan University, Cairo, Egypt
[47]Also at Italian National Agency for New Technologies, Energy and Sustainable Economic Development, Bologna, Italy

[48]Also at Centro Siciliano di Fisica Nucleare e di Struttura Della Materia, Catania, Italy
[49]Also at Università degli Studi Guglielmo Marconi, Roma, Italy
[50]Also at Scuola Superiore Meridionale, Università di Napoli 'Federico II', Napoli, Italy
[51]Also at Fermi National Accelerator Laboratory, Batavia, Illinois, USA
[52]Also at Laboratori Nazionali di Legnaro dell'INFN, Legnaro, Italy
[53]Also at Università di Napoli 'Federico II', Napoli, Italy
[54]Also at Ain Shams University, Cairo, Egypt
[55]Also at Consiglio Nazionale delle Ricerche - Istituto Officina dei Materiali, Perugia, Italy
[56]Also at Riga Technical University, Riga, Latvia
[57]Also at Department of Applied Physics, Faculty of Science and Technology, Universiti Kebangsaan Malaysia, Bangi, Malaysia
[58]Also at Consejo Nacional de Ciencia y Tecnología, Mexico City, Mexico
[59]Also at Trincomalee Campus, Eastern University, Sri Lanka, Nilaveli, Sri Lanka
[60]Also at Saegis Campus, Nugegoda, Sri Lanka
[61]Also at INFN Sezione di Pavia, Università di Pavia, Pavia, Italy
[62]Also at National and Kapodistrian University of Athens, Athens, Greece
[63]Also at Ecole Polytechnique Fédérale Lausanne, Lausanne, Switzerland
[64]Also at University of Vienna Faculty of Computer Science, Vienna, Austria
[65]Also at Universität Zürich, Zurich, Switzerland
[66]Also at Stefan Meyer Institute for Subatomic Physics, Vienna, Austria
[67]Also at Laboratoire d'Annecy-le-Vieux de Physique des Particules, IN2P3-CNRS, Annecy-le-Vieux, France
[68]Also at Near East University, Research Center of Experimental Health Science, Mersin, Turkey
[69]Also at Konya Technical University, Konya, Turkey
[70]Also at Izmir Bakircay University, Izmir, Turkey
[71]Also at Adiyaman University, Adiyaman, Turkey
[72]Also at Necmettin Erbakan University, Konya, Turkey
[73]Also at Bozok Universitetesi Rektörlügü, Yozgat, Turkey
[74]Also at Marmara University, Istanbul, Turkey
[75]Also at Milli Savunma University, Istanbul, Turkey
[76]Also at Kafkas University, Kars, Turkey
[77]Also at Hacettepe University, Ankara, Turkey
[78]Also at Istanbul University - Cerrahpasa, Faculty of Engineering, Istanbul, Turkey
[79]Also at Yildiz Technical University, Istanbul, Turkey
[80]Also at Vrije Universiteit Brussel, Brussel, Belgium
[81]Also at School of Physics and Astronomy, University of Southampton, Southampton, United Kingdom
[82]Also at University of Bristol, Bristol, United Kingdom
[83]Also at IPPP Durham University, Durham, United Kingdom
[84]Also at Monash University, Faculty of Science, Clayton, Australia
[85]Now at an institute or an international laboratory covered by a cooperation agreement with CERN
[86]Also at Università di Torino, Torino, Italy
[87]Also at Bethel University, St. Paul, Minnesota, USA
[88]Also at Karamanoğlu Mehmetbey University, Karaman, Turkey
[89]Also at California Institute of Technology, Pasadena, California, USA
[90]Also at United States Naval Academy, Annapolis, Maryland, USA
[91]Also at Bingol University, Bingol, Turkey

[92]Also at Georgian Technical University, Tbilisi, Georgia
[93]Also at Sinop University, Sinop, Turkey
[94]Also at Erciyes University, Kayseri, Turkey
[95]Also at Horia Hulubei National Institute of Physics and Nuclear Engineering (IFIN-HH), Bucharest, Romania
[96]Also at Texas A&M University at Qatar, Doha, Qatar
[97]Also at Kyungpook National University, Daegu, Korea
[98]Also at another institute or international laboratory covered by a cooperation agreement with CERN
[99]Also at Universiteit Antwerpen, Antwerpen, Belgium
[100]Also at Yerevan Physics Institute, Yerevan, Armenia
[101]Also at Northeastern University, Boston, Massachusetts, USA
[102]Also at Imperial College, London, United Kingdom
[103]Also at Institute of Nuclear Physics of the Uzbekistan Academy of Sciences, Tashkent, Uzbekistan